



Published in final edited form as:

Adv Drug Deliv Rev. 2010 August 30; 62(11): 1064–1079. doi:10.1016/j.addr.2010.07.009.

Nanoparticle-based theranostic agents

Jin Xie, Seulki Lee, and Xiaoyuan Chen

Laboratory of Molecular Imaging and Nanomedicine, National Institute of Biomedical Imaging and Bioengineering, National Institutes of Health, 31 Center Dr, Suite 1C14, Bethesda, MD 20892-2281

Abstract

Theranostic nanomedicine is emerging as a promising therapeutic paradigm. It takes advantage of the high capacity of nanoplateforms to ferry cargo and loads onto them both imaging and therapeutic functions. The resulting nanosystems, capable of diagnosis, drug delivery and monitoring of therapeutic response, are expected to play a significant role in the dawning era of personalized medicine, and much research effort has been devoted toward that goal. A convenience in constructing such function-integrated agents is that many nanoplateforms are already, themselves, imaging agents. Their well developed surface chemistry makes it easy to load them with pharmaceuticals and promote them to be theranostic nanosystems. Iron oxide nanoparticles, quantum dots, carbon nanotubes, gold nanoparticles and silica nanoparticles, have been previously well investigated in the imaging setting and are candidate nanoplateforms for building up nanoparticle-based theranostics. In the current article, we will outline the progress along this line, organized by the category of the core materials. We will focus on construction strategies and will discuss the challenges and opportunities associated with this emerging technology.

Keywords

Theranostics; drug delivery; gene delivery; nanomedicine; molecular imaging; iron oxide nanoparticles; quantum dots; gold nanoparticles; carbon nanotubes; silica nanoparticles

1. Introduction

The term “theranostics” was coined to define ongoing efforts in clinics to develop more specific, individualized therapies for various diseases, and to combine diagnostic and therapeutic capabilities into a single agent. The rationale arose from the fact that diseases, such as cancers, are immensely heterogeneous, and all existing treatments are effective for only limited patient subpopulations and at selective stages of disease development. The hope was that a close marriage of diagnosis and therapeutics could provide therapeutic protocols that are more specific to individuals and, therefore, more likely to offer improved prognoses.

The emergence of nanotechnology has offered an opportunity to draw diagnosis and therapy closer. Nanoparticle (NP)-based imaging and therapy have been investigated separately, and

For correspondence: Xiaoyuan Chen, PhD Phone: (301) 451-4246, Fax: (301) 480-1613, Shawn.Chen@nih.gov. Seulki Lee, PhD, Phone: (301)-402-3427, Fax: (301)-480-5444, seulki.lee@nih.gov.

Publisher's Disclaimer: This is a PDF file of an unedited manuscript that has been accepted for publication. As a service to our customers we are providing this early version of the manuscript. The manuscript will undergo copyediting, typesetting, and review of the resulting proof before it is published in its final citable form. Please note that during the production process errors may be discovered which could affect the content, and all legal disclaimers that apply to the journal pertain.

understanding of them has now evolved to a point enabling the birth of NP-based theranostics, which can be defined as nanoplatforms that can co-deliver therapeutic and imaging functions. This is in a way an extension of the traditional theranostics but focusing more on “co-delivery”. It adds to the previous paradigm for allowing imaging to be performed not only before or after, but also during a treatment regimen. It is convenient that many nanomaterials are already imaging agents and can be readily “upgraded” to theranostic agents by mounting therapeutic functions on them. One underlying driving force of such a combination is that imaging and therapy both require sufficient accumulation of agents in diseased areas. This common targeting requirement brings the two research domains closer and, ultimately, will blur the boundary between them, since many techniques to enhance imaging can, at least in theory, be readily transferred to the therapeutic domain, and vice versa.

Targeting strategies can be varied immensely to suit the desired targets. In the case of cancer, it is a common approach to identify a biomarker that is aberrantly expressed on the surface of cancer cells, and then to load its cognate binding vector onto probes/carriers to achieve recognition and tumor homing. For nanoplatforms, the unique size scale of the particles enables achievement of an enhanced-permeability-and-retention (EPR) effect in tumor targeting. In all efforts, however, care has to be taken with the particles’ surfaces to avoid innate immunosystem recognition and to secure sufficiently long circulation half lives for the agents to reach their targets.

Nanoparticle-based imaging and therapy are each struggling to advance into clinical trials and, as descendants of the two, nanoparticle-based theranostics are still in their early stages of development. However, the push provided by advances in nanotechnology and the call for personalized medicine have already made nanoparticle-based theranostics a research hotspot. This review attempts to give a summary of the efforts made so far along this line. We will introduce theranostic agents, arranged by the category of their core nanomaterial, that hold potential in the theranostic setting. The techniques used to form linkage between nanoplatforms and functionally entities have been well developed and are summarized in Table 1. As mentioned above, most of the nanoplatforms to be described here already perform imaging functions and have been widely investigated for imaging related applications. However, imaging alone, without therapy, will not be the focus of this article, and readers are referred to several excellent reviews on that topic. Instead, we will focus on the build-up and application of theranostic agents, as well as the associated surface coating and coupling chemistry that may affect transport, delivery and release of cargos.

2. Iron oxide nanoparticle based theranostic agents

2.1 Preparation and surface chemistry of iron oxide nanoparticles

Iron oxide nanoparticles (IONPs) are nanocrystals made from magnetite or hematite. Despite spin surface disorders and spin canting effect, IONPs typically possess substantial saturation magnetization (M_s) values at room temperature, especially for those made from pyrolysis protocols with good crystallinity. Unlike the bulk materials, IONPs less than 20 nm are superparamagnetic—a state where particles show zero magnetism in the absence of an external magnetic field, but can become magnetized when there is one. The underlying mechanism is that at such small scale, the thermal energy is sufficient to overcome the anisotropy energy of each small magnet (nanoparticle), and this leads to random fluctuation of the magnetizations that, macroscopically, result in zero net coercivity and magnetic moment.

The superior magnetic properties of IONPs, along with their inherent biocompatibility and inexpensiveness, have made IONPs a material of choice in many bioapplications, such as

contrast probes for magnetic resonance imaging (MRI). The high magnetic moments of IONPs make them effective in reducing T2 relaxation time, leading to signal attenuation on a T2 or T2* weighted map. When the particles are engineered with targeting specificity, such signal alterations can be harnessed to report abnormal biological activity.

The synthesis of IONPs has been well documented. Traditionally, IONPs are made in aqueous solution by co-precipitating Fe(II) and Fe(III) precursors. In order to confer colloidal suspendability to the particles, additives, typically hydrophilic polymers, are added during the particle formation process, which passivate the nanocrystal surface and protect against particle aggregation. A number of ligands including polyvinylpyrrolidone (PVP), dendrimer, polyaniline and dextran have been utilized for such purposes, with dextran and its derivatives being the most studied. As a matter of fact, several dextran-IONP formulas have entered or already passed clinical trials as MRI contrast agents. For instance, Feridex particles (AMAG Pharmaceuticals) are FDA approved for the detection of liver and spleen lesions, and their analog Combidex has entered into phase III clinical trial for lymph node imaging. In addition to helping improve colloidal stability of the particles, the polymer coating offers multiple chemical groups that are essential for the coupling of functional species. For instance, we have prepared polyaspartic acid (PASP) coated IONPs and coupled onto the particles RGD and ^{64}Cu -DOTA for positron emission tomography (PET)/MRI dual imaging. Lee et al. have converted dextran-IONPs aminated with epichlorohydrin and ammonia, after which the particles can be readily conjugated with a wide range of biospecies.

Recently, high temperature decomposition has emerged as a useful strategy in nanoparticle preparation. Unlike traditional methods, where aqueous solution is used as the reaction medium, such pyrolysis synthesis takes place in organic solvent upon high temperature treatment. Due to the existence of highly concentrated surfactant ligands, the particle growth is carried out in a controlled fashion, and the resulting IONPs typically possess better crystallinity and higher magnetism than those made from the traditional methods. More importantly, such pyrolysis methods permit accurate control of the products, down to one nanometer size. This is significant because particle size and magnetic properties are tightly associated, and by tuning the reaction parameters, it is therefore possible to achieve a series of IONPs with controllable T2 contrast effects.

One disadvantage of pyrolysis-produced IONPs, however, is that the as-synthesized products are imbedded within a thick alkyl coating and are not water soluble. Many efforts have since been devoted to developing surface modification technologies that can confer conjugatability and water solubility to the particles. Despite their diversity, these surface modification techniques can be generally divided into two categories: ligand exchange and ligand addition. The prior refers to the strategy of using high affinity, hydrophilic ligands to replace the original hydrophobic coating. The latter refers to the use of amphiphilic materials, which are added to the particle surface by forming a bilayer structure with the existing alkyl coating.

2.2 Review of IONP based theranostic agents

IONPs with appropriate coatings can be easily coupled with drug molecules. For instance, the Zhang group coupled methotrexate (MTX), an anti-cancer drug, onto an aminated IONP surface. *In vitro* studies demonstrated that the particles, after internalizing into cells, accumulated in lysosomes, where the drug molecules were released due to the low pH and the presence of proteases. Hwu et al. reported on coupling paclitaxel (PTX) to IONP surfaces through a phosphodiester moiety at the (C-2')-OH position. The average number of PTX molecules per nanoparticles was evaluated to be 83, and the release of the PTX was found to be more effective when exposed to phosphodiesterase. The Cheon group used

meso-2,3-dimercaptosuccinic acid (DMSA) to modify IONPs, and used SMCC as the crosslinker to couple Herceptin antibody molecules onto the particle surface, although Herceptin was harnessed as a targeting agent rather than a therapeutic agent in the study.

Aside from covalent coupling, drug molecules can also be co-capsulated with IONPs into polymeric matrices. Jain et al. loaded doxorubicin (DOX) and PTX, along with oleic acid coated IONPs, into pluronic-stabilized nanoparticles. Similarly, Yu et al. loaded DOX into anti-biofouling polymer coated IONPs. When applied in a Lewis lung carcinoma xenograft model, such DOX loaded nanoconjugates showed better pharmacokinetics and therapeutic effects than DOX alone, presumably due to the anti-biofouling feature of the particles. Similarly, protein molecules have also been investigated as drug carriers. For instance, we developed a two-step coating strategy to yield human serum albumin (HSA) coated IONPs. With the excellent binding capacity of HSA, we expect that a range of lipophilic pharmaceuticals can be loaded into such nanoplatforms to yield theranostic agents.

It is known that small molecules can be loaded into porous nanostructures via physical absorption and, along that line, there have been efforts to achieve hollow iron oxide nanostructures. One such effort was reported by the Hyeon group. Starting from spindle-shaped β -FeOOH NPs made from FeCl_3 hydrolysis, they performed a three step, so-called “wrap-bake-peel” treatment to achieve hollow IONPs. In a proof-of-concept study, they found that DOX could be loaded into such hollow nanoparticles via simple physical absorption and then released from the nanostructures in a sustained manner under physiologic conditions. A more recent report was given by the Sun group. By controlled oxidation and acid etching of Fe particles, they were able to achieve porous IONPs with a sizable cavity. They then loaded cisplatin into the cavities of the particles, and coupled Herceptin onto the particle surfaces to confer targeting specificity. The resulting conjugates showed selective affinity to ErbB2/Neu-positive breast cancer cells and a sustained cytotoxicity attributable to the controlled release of cisplatin from the particle carriers.

Gene therapy has emerged as a crucial therapeutic avenue, where DNAs/RNAs are utilized as therapeutics to antagonize abnormal gene regulation. Unlike small-molecule-based therapeutics, DNAs/RNAs are negatively charged and, by themselves, have difficulty passing through the negatively charged cell membrane. In addition, the nucleases that are ubiquitous in living subjects may recognize and degrade DNAs/RNAs before they reach their targets and fulfill their task. It is in this scenario that nanoparticle-based delivery plays a significant role. In an ideal situation, the nanoparticle carriers can load the therapeutic genes, escort them to the diseased areas, facilitate their shuttling across the target cell membranes and, finally, release them intracellularly and fulfill their functions.

A milestone work along this line was reported by Medarova and his colleagues (Fig. 1). They coupled thiolated siRNA onto aminated dextran particles using N-succinimidyl-3-(2-pyridyldithio) propionate (SPDP) as a bridge compound. In addition, the near infrared dye Cy5.5 and myristoylated polyarginine peptide (MPAP), a membrane translocation peptide, were coupled to the particle surface. The probes were first equipped with siRNA that targets green fluorescence protein (GFP), and the conjugates were tested in a mouse model bearing bilateral 9L-GFP and 9L-RFP tumors. MRI and near-infrared fluorescence (NIRF) imaging were performed, and appreciable probe accumulation was found in both tumors. In contrast, optical signal drop was only observed in the 9L-GFP tumor, and not in the 9L-RFP tumor. siRNA-GFP was then switched to a therapeutic siRNA sequence that targets the antiapoptotic gene *Birc5* (which encodes the protein survivin), and studied the therapeutic potential of the nanoconjugate in an LS174T human colorectal carcinoma xenograft model. RT-PCR results showed that such therapeutic particles induced an amazing drop in survivin

transcript level of $97 \pm 2\%$, accompanied by increased levels of tumor-associated apoptosis and necrosis.

In the above study, the particle accumulation in tumor was mediated by the EPR effect. It is also possible to add biovectors to nanoplatfoms in order to impart site-specific delivery. For instance, Cheon group coupled siRNA and a PEGylated cyclic Arg-Gly-Asp (RGD) peptide onto magnetic nanoparticles. In a proof-of-concept study, MDA-MB-435 and A549 cells, which have high and negative integrin $\alpha_v\beta_3$ expression, respectively, were stably transfected with GFP and were incubated with nanoparticles loaded with GFP siRNA. The two cell lines showed distinct particle internalization rates, confirming that the particle uptake was mainly mediated by RGD-integrin interaction. Such differences in uptake resulted in a dramatic discrepancy in gene regulation efficacy. While the particles alone, with or with RGD coupling, showed no effect on knocking down GFP expression in A549 cells, a significant and concentration-dependent decrease in GFP expression was observed with MDA-MB-435 cells.

The magnetic properties of IONPs allow them to accumulate upon the summons of an external magnetic field. This feature has been utilized as a targeting mechanism to improve drug delivery efficiency, and related studies in animals and in human have been reported. In one such study, seven patients with metastatic breast cancer were infused with epirubicin-loaded IONPs (100 nm in diameter, at 0.5% of the estimated blood volume), and after that a magnetic field was established around the tumor. In about half of the patients, the magnetic field proved successful in directing the ferrofluid to the tumor to induce tumor regression. In a very recent effort, Namiki et al. screened cationic lipid coated IONPs, and found one formula, designated as LipoMag, that outperformed commercial PolyMag in both transfection and gene knockdown in all 13 tested cell lines (Fig. 2). The authors also screened and found the one sequence, siRNA^{EGFR#4}, with the maximum percentage knockdown of EGFR mRNA. They then performed 2'-OMe modification on the uridine residues of the sense strand and yielded a modified sequence with similar knockdown effect but reduced cytokine induction compared with the parent sequence. Subsequently, they loaded this modified siRNA onto nanoparticles and evaluated their therapeutic potency in two gastric cancer models. A 50% reduction in tumor volume was observed in the therapeutic group after a 28-day treatment, along with other desired events, such as inhibition of angiogenesis and induction of apoptosis. Notably, such gene knockdown was only significant during application of magnetic fields at the tumor sites, as the lipid particles alone were not an effective delivery vehicle.

IONP can itself play an imaging/therapy dual role, due to its potential in hyperthermia. The underlying mechanism is that IONPs can act as antennae in an external alternating magnetic field (AMF) to convert electromagnetic energy into heat. This feature holds promise in tumor therapy for tumor cells that are more susceptible to elevated temperature than normal cells. In one example, phospholipid coated IONPs were injected into a subcutaneous tumor model in F344 rats, and were exposed to an AMF. The AMF in conjugation with IONPs raised the temperature of tumor above 43 °C and caused tumor regression, but had no effect on the control group where no IONPs were given. Also, Fab fragment of anti-human MN antigen-specific antibody was chemically anchored onto IONP surfaces and the IONPs were administrated systemically into tumor-bearing mice. The particles showed high tumor uptake, presumably due to an antibody-antigen interaction, and induced efficient tumor hyperthermia when exposed to an AMF. In another study, Zn-Pc, a photodynamic therapeutic (PDT) agent, was loaded onto CoFe₂O₄ nanoparticles, which showed better hyperthermia effects than IONPs. When evaluated *in vitro* with J774-A1 macrophage cells, a combined toxicity from both PDT and magnetohyperthermia was observed; however, more work needs to be done to elucidate the synergy of such combinational *in vivo* therapy.

3. Quantum dot based theranostic agents

3.1 Preparation and surface chemistry of quantum dots

Quantum dots (QDs) are light-emitting nanocrystals made from semiconductor materials. QDs are becoming an important class of biomaterials, because they possess unique optical properties that are unavailable from organic dyes or fluorescent proteins, such as being brighter, more photo- and chemical stable and possessing a narrow emission spectrum.

A unique feature of QDs is that their optical properties can be accurately adjusted by tuning their size and composition. The first generation of QDs was made of CdSe, CdTe and PbS, and by tuning of their sizes, gave rise to a series of nanomaterials that span most of the visible spectrum. However, such materials were found inefficient in *in vivo* applications due to the limited tissue penetration distances of visible light. To address this issue, exploits for QD formulas with near-infrared emission have been made, and those composed of CdTe/CdSe, Cd₃P₂, InAs/ZnSe and InAs/InP/ZnSe have been reported. An inorganic coating, such as ZnS, is usually added to the particle surface, and this has proved useful in enhancing the photoluminescent quantum efficiencies of the particles.

The synthesis of QDs is reminiscent of IONP preparation. In brief, appropriate organometallic precursors are heated in high boiling point organic solvent to initiate particle formation. Surfactants, such as trioctylphosphine (TOP) and trioctylphosphine oxide (TOPO), are utilized to control the particle growth. Similar to IONP synthesis, as-synthesized QDs are alkylated and are not water soluble. To confer water solubility, the most straightforward strategy is to add thiolated species to form disulfide linkage with the QD core or the ZnS shell. A host of small thiolated molecules have been investigated for such purposes, including mercaptoacetic acid, mercaptopropionic acid, mercaptosuccinic acid, dithiothreitol, glutathione, dithiothreitol (DTT) and cysteine. Interestingly, such old-school techniques have recently reentered scientific evaluations to prepare QDs with a minimized hydrodynamic size. A milestone finding has been that, when modified with cysteine, QDs can be rendered water soluble with a hydrodynamic size less than 5.5 nm and, when administrated systemically, these QDs have been found to be rapidly excreted via renal clearance, rather than being trapped in reticuloendothelial system (RES) organs, such as liver and spleen, as has been observed with most other nanoformulas. More recently, InAs/InP/ZnSe QDs have been coated with mercaptopropionic acid with an overall size of 8 nm, and intravenous injection in mice showed appreciable renal clearance that was confirmed by both NIRF imaging and urine sample assessment. One common concern of such a modification technique is the fragility of the disulfide bond. To strengthen the linkage, polydentate ligands, such as DHLA, oligomeric phosphines, cysteine rich peptides or multidentate polymers have been investigated, and they have been able to improve the longevity of the nanostructures. On the other hand, although it is S of the ZnS layer that is mostly utilized as a species-mounting site, it was reported that proteins/peptides with poly-histidine tags can be efficiently anchored onto QDs via strong Zn(II)-His interaction.

In addition to ligand-exchange, efforts have been made to investigate ligand-addition-based surface modification techniques, which involved a group of amphiphilic compounds, such as phospholipids, amphiphilic saccharides, acrylic acid polymers and others. One pioneering study was reported by Nie and his colleagues, who utilized a triblock copolymer (consisting of a polybutylacrylate segment, a polyethylacrylate segment, a polymethacrylic acid segment and a hydrophobic hydrocarbon side chain) to modify QDs and conjugated onto them a prostate-specific membrane antigen (PSMA) targeting antibody. When administrated into prostate cancer bearing mice, the nanoconjugates accumulated in the tumor area. This accumulation was attributed to both the EPR effect and specific antibody-antigen interaction.

3.2 Review of quantum dot based theranostic agents

QD based drug delivery is relatively less investigated, largely due to the innate toxicity of QDs. This problem is more prominent with the first generation QDs, where toxic Cd and Pb are frequently used in QD preparation. Recent advances in QD synthesis have led to the emergence of Cd-free QDs, such as InAs/ZnSe and InAs/InP/ZnSe. They are potentially more qualified candidate carriers, but relevant applications are so far limited. Nonetheless, Nurunnabi et al. reported on making QDs-Herceptin conjugates. The CdTe/CdSe QDs were made water soluble through the addition of PEG-10,12-pentacosadiynoic acid (PEG-PCDA), and the nanostructure was further stabilized upon UV irradiation, which crosslinked the coating shell and helped reduce the risk of Cd²⁺ leaking out from the core materials. The nanoparticles showed an efficient tumor targeting rate and impressive therapeutic effects when tested on an MDA-MB-231 tumor model. Park et al. co-encapsulated hydrophobic QDs and IONPs, along with DOX, into micelles formed with PEGylated phospholipid. Such conjugates were further coupled with a tumor-homing peptide F3, and were injected into an MDA-MB-435 xenograft model. Successful tumor targeting was observed by both optical and MR imaging modalities and was attributed to the mediation of the tumor-homing peptide. However, as a proof-of-concept study, the investigation stopped at the imaging level and no therapeutic studies were pursued.

In another interesting study, Bagalkot et al. produced a QD-aptamer(Apt)-DOX conjugate [QD-Apt(Dox)], and investigated its use for simultaneous cancer imaging, therapy and therapy monitoring (Fig 3). A10 RNA aptamer was coupled to the QD surface and was utilized as a biovector to target PSMA. The DOX loading, on the other hand, was achieved by its intercalation within the aptamer sequence. Interestingly, the fluorescence activities from QD and DOX were attenuated by their interaction with DOX and RNA, respectively, and were both in a quenched state in the nanosystem. However, when the particles were delivered into targeted tumor cells, DOX would be gradually released from the system, which, aside from initiating therapeutic functions, also led to the recovery of QD fluorescence. Similarly, Yuan et al. loaded MTX onto QD surfaces to induce photoluminescence quenching. The loading was achieved via simple reversible physical adsorption, which can be reversed when exposed to species with higher affinity, such as DNA. This coating change led to a restoration of the photoluminescence, which can be potentially useful to monitoring the delivery of drug molecules.

QDs may also function as gene delivery vehicles when modified with lipofectamine or other positively charged polymers. For instance, QDs have been encapsulated in poly(maleic-anhydride-alt-1-decene), and further surface-modified with dimethylamino propylamine to be positively charged. The resulting QDs outperformed polyethylenimine (PEI) by showing more efficient delivery and significantly reduced toxicity. Also with poly(maleic-anhydride-alt-1-decene) coated QDs, Gao et al. converted some carboxyls to tertiary amines with N,N-dimethylethylenediamine. The resulting particles, possessing two functional groups on the particle surface, afforded both steric and electrostatic interactions that were highly responsive to acidic endosome/lysosome organelles. When assessed as siRNA delivery vehicles, such QDs showed a 10–20 fold increase in silencing effect and a 5–6 fold decrease in toxicity when compared with other common delivery agents, such as lipofectamine, JetPEI and TransIT. Covalently coupling siRNA to QDs has been investigated in addition to loading siRNA via electrostatic force. Derfus et al. covalently conjugated siRNA, along with a tumor-homing peptide F3, onto QDs. To study the feasibility of siRNA release, the coupling was achieved via two routes: with disulfide cross-linker and by forming a non-reducible, thioether linkage. Using eGFP as the target, it was shown that the former formula had greater gene silencing efficiency, which the authors attributed to the susceptibility of disulfide linkage in endosome/lysosome. More recently, QDs modified with amine functionalized polymer polydiallyldimethylammonium chloride

(PDDAC) have been complexed with MMP-9-siRNA and utilized to modulate the activity of MMP-9, a main component of the blood brain barrier (BBB), in brain microvascular endothelial cells (BMVEC). The treatment caused an increase in the expression level of tissue inhibitor of metalloproteinase-1 (TIMP-1), a natural inhibitor of MMP-9 that functions to maintain the basement membrane integrity. In parallel, increases in collagen I, IV, V expression and a decrease in endothelial permeability were also observed.

QDs also have great potential in photodynamic therapy, where they act as either photosensitizers themselves or as carriers. The underlying mechanism for the first paradigm is that QDs can be activated by light and transfer the triplet state energy to nearby oxygen molecules to cause cell damage. Tsay et al. modified QDs with streptavidin and conjugated onto them biotinylated pDNA. They found the generation of reactive oxygen intermediates (ROI), through nitroblue tetrazolium (NBT) assay, when the QDs were photoactivated. Further investigation found that such ROI can elicit damage to purine and pyrimidine bases, as was confirmed by assays with base excision repair enzymes, such as formamidopyrimidine glycosylase (Fpg) and endonuclease III (Endo III). Compared with small-molecule-based photosensitizers, such QD based PDT offers advantages, such as better chemical stability, water solubility, and (for NIRF QDs) less optical interference with biological tissues. The drawback, however, is that the quantum yield of such QD-generated singlet oxygen is typically less than 5%, much lower than that of classic photosensitizers (40–60%).

QDs have also been investigated as carriers for PDT agents. Hsieh et al. conjugated QDs with Ir-complex. Samia et al. conjugated QDs with phthalocyanine (Pc4). Shi et al. used meso-tetra(4-sulfonatophenyl)porphine dihydrochloride (TSPP) as a photosensitizer and coupled it onto QD surfaces. Note that, in the latter two cases, the QDs worked as drug carriers and were not directly involved in the photodynamic therapy. In Samia's system, however, the QD also worked as an energy hub, which transferred energy to phthalocyanine (Pc4) to activate its PDT function.

The use of QDs for biomedical application arises from their unique physicochemical properties, including broad absorption spectra, size-dependent narrow and stable emissions spectra, photostability, and the ability to serve as scaffold for additional agents such as targeting ligands and therapeutic drugs. In addition, there are numerous unexplored possibilities to expand the use of QD-based theranostic agents based on its multiplexing and FRET capabilities. However, there is an urgent need to understand the metabolism of QDs in the body and address the heavy metal related toxicity issues.

4. Gold nanoparticle based theranostic agents

4.1 Preparation and surface chemistry of gold nanoparticles

Gold nanoparticles (Au NPs) possess many unique features and have been investigated in a variety of imaging related arenas, such as in computed tomography (CT), photoacoustics and surface-enhanced Raman spectroscopy (SERS). Synthesis of Au NPs has been well established, and those in the forms of spheres, cubes, rods, cages and wires can now be acquired with accurate quality control and in large quantity. Such morphology control is important as it greatly influences the physical properties of the products and in turn affects their role as imaging probes. For instance, 10 nm spherical Au NPs have characteristic surface plasmonic absorption at around 520 nm. Increasing the particle size leads to some, but not dramatic, red-shift of the particle absorption spectrum--the maximum absorption of 48.3 and 99.4 nm Au NPs are at 533 nm and 575 nm, respectively. Changing the nanoparticle shape to rod-like, on the other hand, can push the absorption to the NIR region

(650–900 nm), which suggests their role as probes in photoacoustic imaging or mediators in photothermal therapeutics.

Due to the strong interaction between thiol and Au, the surface modification of Au nanostructures is overwhelmingly conducted via addition of thiolated species. Typically, a bifunctional compound is utilized, which has its thiol termini immobilized onto the particle surface, while leaving carboxyl/amine termini exposed for conjugation with functional entities. Alternatively, biomolecules can be pre-thiolated and loaded as a whole onto particles. For instance, thiolated DNA oligos have long been utilized for stabilizing Au NP colloids and the resulting conjugates have been investigated as gene therapy agents. Unlike surface modification of QDs, where the fragility of disulfide binding is a concern, a monodentate thiol is generally regarded sufficient to induce stable ligand anchoring of Au. As a matter of fact, monodentate ligands can be more advantageous than multidentate species to allow higher loading capacity. This is evidenced by a study where two oligonucleotides -- one tetrathiol modified and the other monothiol modified--were loaded onto separate 13 nm Au NPs. Although the tetrathiol oligos and the monothiol oligos shared the same sequence, only 45~50 tetrathiol strands can be loaded onto each particle, compared to 110~120 for monothiol oligos.

In the nanorod synthesis, cetrimonium bromide (CTAB) is widely used. It works by forming a thick double-layer around the side wall of the nanorods, and causes a longitudinal growth of the nanostructure. Thus, most thiol-Au interaction occurs at the ends of the nanorods, since the side wall is hard to access. In order to achieve a better loading rate, a layer-by-layer deposition approach is sometimes utilized. This method takes advantage of the highly positively charged CTAB coating and loads alternatively charged species to the particle surface. In such a manner, large functional molecules, such as antibodies, can be directly immobilized onto the outer layer of the particle surface with electrostatic interaction.

4.2 Review of gold nanoparticle based theranostic agents

As already mentioned, Au-thiol chemistry is favored to load functional entity onto Au NPs, and a number of therapeutics have been loaded in such manner. For instance, PTX was modified at its C-7 position and covalently coupled to 4-mercaptophenol modified Au nanoparticles. The resulting conjugates demonstrated better therapeutic effects than MTX alone both *in vitro* and *in vivo*, which was likely due to the “concentrated effect” and an improved pharmacokinetics of the conjugates. Similarly, protein based pharmaceuticals have been loaded onto Au NPs. Tumor necrosis factor (TNF), for instance, was coupled to PEGylated Au nanoparticles, and the resulting conjugates showed better therapeutic efficacy and less toxicity than native TNF.

In addition to thiol-Au association, other ways of anchoring pharmaceuticals have also been investigated. Pokharkar et al. used chitosan as a reducing agent and coating material to make Au nanoparticles. The resulted chitosan-Au nanoparticles were highly positively charged and were found highly efficient in loading insulin via electrostatic interaction (53%). Such conjugates were studied in a diabetic model to control postprandial hyperglycemia. Two hours after administrating these insulin loaded Au NPs to diabetic rats, a drop in their blood glucose level was observed, of 30.41% and 20.27% for oral (50 IU/kg) and nasal (10 IU/kg) administration, respectively. Cheng found that a PDT agent, Pc4, can be directly adsorbed onto PEGylated Au nanoparticles with high efficiency. The Au nanoparticles worked well as a drug carrier, reducing the time for sufficient Pc4 delivery to less than 2 h, compared to that of 2 days for free drug. Similar work with zinc-Pc was reported by Hone et al.. Prabaharan et al. utilized an amphiphilic-block-copolymer-coated Au NP formula for tumor targeting and drug delivery. Such a nanostructure consisted of a Au NP core, a hydrophobic PASP inner shell, and a hydrophilic, folate-conjugated PEG outer shell (PEG-OH/FA). DOX was

covalently conjugated onto the hydrophobic inner shell by acid-cleavable hydrazone linkage, with a loading level of 17 wt%. Such a nanosystem is interesting for possessing both a tumor targeting mechanism (folate on the outer layer) and an intracellular drug release mechanism (hydrazone linkage of DOX on the inner layer).

Au NPs have also been converted to polyelectrolytes and studied as gene delivery carriers. Previously, Au NPs have been functionalized with alkylated quaternary ammonium to load plasmid DNA. *In vitro*, such nanocarrier showed benefits such as protecting DNA from enzymatic digestion and GSH activated release. Later, Klivanov et al. used branched PEI to confer gene loading capacity to Au NPs. Under optimized conditions, transfection potency can be increased by 12 times, compared to the parent polymer. In addition to electrostatic forces, therapeutic genes can also be loaded onto Au nanoparticles through covalent linking. As mentioned above, thiolated antisense DNA oligos can be directly loaded onto Au nanoparticles with high efficiency. In a cellular study with eGFP-expressing C166 cells, Au NPs loaded with antisense DNA showed a high translocation rate and a prominent gene knockdown efficiency.

The unique surface plasmon resonance feature of Au NPs makes them candidate materials in photothermal therapy. The idea is to use Au NPs to serve as energy transducers, which, when concentrated in tumor areas and upon laser irradiation, can convert light into heat and kill adjacent cancerous cells. Compared with conventional drug delivery, such a treatment paradigm is active only within the limited illumination area, therefore minimizing normal tissue damage. As mentioned above, spherical Au NPs, with a characteristic absorption at 500–600 nm, are not appropriate materials for such an application. Changing the configuration to a nanorod, nanocage or nanoshell, on the other hand, can shift the absorption to the NIR region, and reports on gold-nanostructure-based hyperthermia are accumulating. For instance, the Xia group demonstrated recently that PEG coated Au nanocages can accumulate in a U87MG xenograft model, and when exposed to NIR light, can increase the tumor surface temperature to 54 °C within 2 min. Li coupled α -melanocyte-stimulating hormone (MSH) analog, [Nle⁴, D-Phe⁷] α -MSH (NDP-MSH), onto Au nanoshells and administrated such conjugates to a B16/F10 melanoma model (Fig 4). Careful histological examination found high accumulation of particles in the tumor and confirmed that such homing was mediated by NDP-MSH. Efficient ablation of B16/F10 melanoma was found in the tumor exposed to laser illumination, but not in the contralateral tumor where no illumination was given. Successful photothermal therapy was validated histologically and, more interestingly, [¹⁸F] fluorodeoxyglucose (¹⁸F-FDG) PET found a remarkable decrease in tumor uptake, reflecting a metabolic activity drop upon photothermal therapy. More recently, the same group reported the use of Au nanoshells as light-controllable siRNA carriers (Fig 5). The particles were conferred with tumor targeting specificity by imparting folic acid to the particle surface. The siRNA, with a sequence that targets NF- κ B P65, was pre-thiolated at the 5' end of the sense chain and was introduced to the particles surface via thiol-Au interaction. It was concluded that the stable thiol-Au association could carry the siRNA payload on the particle surface, even after cell uptake, but would be destroyed when exposed to NIR light irradiation, which damaged the endolysosomal membrane and led to a release of siRNA into cytoplasm. This mechanism of action was confirmed by the observation of light-inducible siRNA release and subsequent NF- κ B P65 downregulation both *in vitro* and *in vivo*. Furthermore, it was found that the downregulation of NF- κ B P65 resulted in increased sensitivity to chemotherapy, as evidenced by an improved therapeutic index when such photothermal therapy was combined with irinotecan treatment.

With unique characteristics, such as strong surface plasmon absorption, stability, biosafety, and ease of modification, AuNP have long been exploited as a candidate material for

building up functional agents for both imaging and therapy applications. One obvious disadvantage is its high cost of production, which may cast a shadow over applications that are otherwise of bright clinical perspectives. Also notably, while the thiol-Au chemistry is convenient and is generally regarded as sufficient to prepare stable AuNP conjugates, it can be an issue when exposed to a reducing environment, such as glutathione (GSH) that is of high concentration in a living subject. While more and more investigations are to be performed at *in vivo* level, new chemistry that are able to result in more stable conjugates can be highly favorable.

5. Carbon nanotube based theranostic agents

5.1 Preparation and surface chemistry of carbon nanotubes

Carbon nanotubes (CNTs) have found potential applications in Raman and photoacoustic imaging and have been studied as drug carriers by a number of research groups. CNTs have a graphite-like structure, which is inert and inhibitive to most conjugation chemistry. To address this issue, researchers have tried to apply extreme oxidative conditions, which generate defects on the CNT surface that can be utilized as mounting sites. For example, after treating single walled nanotubes (SWNTs) in refluxing 2.5 M HNO₃ for two 36 h periods with intervals of 30 min sonication, the SWNTs can be made water soluble due to the generation of multiple carboxyl groups on the nanotube surface. Subsequent conjugation can be applied to covalently link molecules onto those nanotubes by forming amide bonds. Alternatively, it has been reported that azomethine ylide and its derivatives can anchor onto CNT surface through 1, 3-dipolar cyclo-addition. A group of functional molecules, including organic dyes, peptides and antibiotics, have been conjugated to the CNT surface in such a manner.

The hydrophobic and aromatic nature of CNT surface also encourages non-covalent molecule anchoring. Certain amphiphilic compounds, such as sodium dodecyl sulfate (SDS), triton-X-100, CTAB, sodium dodecylbenzene sulfonate (SDBS) and sodium dodecane sulphonic acid (SDSA) have been used to disperse CNT in aqueous solution. One interesting finding is that SDBS is much more efficient than its analog SDS in producing CNT suspension, which has been attributed to the aromatic ring in SDBS that interacts with the CNT surface and further lowers the energy. Indeed, aromatic compounds, such as 1-pyrenebutanoic acid succinimidyl ester, PS-b-PAA and 1-pyrenepropylamine hydrochloride have proved effective in modifying CNTs. Along this line, there have been recent efforts to use DNA oligos to modify CNTs. With multiple bases forming π - π interactions with the graphite surface, the DNA oligos can wrap around the CNT in a helical manner, and disperse the conjugates with the sugar-phosphate backbones exposed to the solution.

Among the many ligands that are available to functionalize the CNT surface, PEGylated phospholipids might be one of the most studied due to its effectiveness and biocompatibility. The Gambhir group conducted a four-month careful monitoring of mice intravenously administered phospholipid coated CNTs. Even though some CNTs were found trapped in the liver and spleen without degradation, no evidence of toxicity was found from the survival, clinical, and laboratory parameters, necropsy and tissue histology studies. Although it is still debatable whether CNT is safe or not for *in vivo* applications, such studies at least suggested a possibility that inconsistent observations in CNT toxicity studies could be caused by the coating materials, rather than the CNTs themselves.

5.2 Review of carbon nanotube based theranostic agents

Carbon nanotubes can be taken up by cells, and this feature has inspired a wave of research efforts to investigate their potential role in drug delivery. The detailed mechanisms underlying such efficient cell penetration are unclear. As a matter of fact, CNTs can be

internalized by cells via different routes, if surface coatings are different and with appropriate coatings, as both endocytosis and passive diffusion have been reported to be responsible for carbon nanotube uptake.

Previously, Prato et al. coupled MTX onto 1, 3-dipolar cycloaddition functionalized CNTs. Similar CNT formulas with multiple amine termini were used to load and deliver DNA plasmid. However, at least in the MTX case, it was found that the covalent amide bond was unfavorable to eliciting intracellular drug release, since the conjugates showed no enhancement in therapeutic efficacy as compared to MTX alone. The Dai group applied phospholipid-CNT conjugates in both imaging and therapy. For example, they coupled siRNA to CNTs via a disulfide bond, which was susceptible to enzymatic breakage in the endolysosome. This CNT transporter showed high transfection efficiency, outperforming lipofectamine in inducing RNAi. Later, they used the same nanostructure and successfully shuttled siRNA into human T cells and primary cells, which are generally regarded as hard to transfect with conventional cationic liposome-based transfection agents. The same group also reported the coupling of either Pt(IV) prodrug or PTX onto PEGylated CNTs to improve the pharmacokinetics and therapeutic effects. In the case of PTX, a branched-PEG was used for phospholipid PEGylation, which was found to be advantageous over single-chain PEG in bringing extra stability to CNTs (Fig 6). PTX was coupled through a cleavable ester bond to the nanotube surface and the construct was then tested in a murine 4T1 breast cancer model. The conjugates showed a 10-fold increase in tumor homing than PTX alone, which was attributed to the prolonged circulation half-life of the nanoformula. Consequently, this formula showed better tumor suppression outcome than clinically used Taxol.

Aromatic stacking can also serve as a drug loading mechanism. DOX, for instance, was loaded onto SWNT via this route at a remarkably high efficiency of 4g DOX/g nanotube. The interaction is pH dependent, suggesting a way of unloading the payloads in acidic endolysosome and tumor micro-environments. More recently, such DOX loaded nanotubes have been evaluated in SCID mice bearing Raji lymphoma xenografts, which showed greater therapeutic efficacy and less toxicity compared to an equimolar amount of free DOX (Fig 6).

The strong optical absorbance of CNTs in the NIR region has made it a promising tool in photothermal therapy. Previous studies have shown that, when irradiated by NIR light, CNTs that were internalized in cells were capable of triggering endosomal rupture and cell death. More recently, Moon et al. demonstrated in a human epidermoid mouth carcinoma model that the combined treatments of PEGylated SWNT and NIR irradiation led to the eradication of tumors with no observation of recurrence over 6 months. Also, Ghosh et al. used DNA to encapsulate CNT, which, according to the authors, can lead to improved heat emission efficacy. When injected in a PC3 xenograft model and irradiated, the conjugates induced complete tumor eradication. However, it is worth pointing out that in both cases the nanotubes were injected intratumorally rather than systemically.

Overall, CNTs have unique physical and surface features and are a key player in the field of nanomedicine. Aside from loading drug molecules, other nanoparticles such as IONPs or AuNPs can be easily tethered on CNTs to further enrich the nanoplatform. However, their non-biodegradability remains to be a great concern. It is debatable whether residual CNTs can cause chronic and longitudinal damage to the host. In addition, there is a lack of a standard protocol to prepare CNTs of high purity and at large scale, which is mandatory for a clinical translation.

6. Silica nanoparticle based theranostic agents

6.1 Preparation and surface chemistry of silica nanoparticles

Silica is generally regarded as a safe material, and has been previously used as surgical implant. It is well documented, as well, that accurate size and morphology control are achievable in the synthesis of silica nanoparticles. Generally, silica nanoparticles themselves do not have characteristics for imaging. Instead, they afford an excellent platform that allows facile loading of a broad range of imaging and therapeutic functions, making them a good candidate for theranostic purposes.

Silica nanoparticles can be formed by hydrolysis and condensation of tetraethyl orthosilicate (TEOS). To introduce functional groups onto the particles, it is very common to use aminopropyltrimethoxysilane (APS) or mercaptopropylmethoxysilane (MPS) as co-precursors, which co-coagulate with the TEOS matrix to bring amine or thiol groups to the particle surface. A functional molecule can be easily imported into the nanosystem during the particle formation, if it is pre-coupled with APS/MPS. Both organic dyes and Gd-DTPA complexes have been coupled and integrated into silica particle matrix through this approach to yield optically or magnetically active agents.

Aside from small molecules, nanoparticles can also be easily incorporated into silica matrices, and reports on using such technology to encapsulate IONPs, Au NPs and QDs have been well documented. Moreover, several functionalities can be encapsulated into a single silica particle simultaneously. For example, Nie et al. utilized silica to encapsulate both IONPs and QDs, creating a hybrid that retained both magnetic and optical properties. Koole et al. reported a dual-function core-shell-shell (CSS) nanoparticle, where silica nanoparticles were loaded with both QDs and Gd complexes.

6.2 Review of silica nanoparticle based theranostic agents

Drug molecules can be easily introduced into silica nanoparticles during particle formation. Roy et al. incorporated 2-devinyl-2-(1-hexyloxyethyl)pyropheophorbide (HPPH), a hydrophobic photosensitizing anticancer drug, into silica matrices. It was demonstrated that the HPPH is more fluorescent in the silica matrices than in the free form, and can efficiently kill cancer cells when irradiated with a laser. Recently, the same group co-encapsulated HPPH and a two-photon absorbing dye, 9,10-bis[4'-(4''-aminostyryl)styryl]anthracene (BDSA), into silica nanoparticles. It was shown that BDSA can efficiently up-convert the NIR light and intrapartically transfer the energy to HPPH to activate the latter's PDT function.

A breakthrough in silica nanoparticle preparation is that they can be made in mesoporous form with accurate pore size control. Such mesoporous nanostructures, consisting of hundreds of empty channels and a large surface area (>900 m²/g), are excellent reservoirs for small molecules and they hold great promise in drug delivery. Many methods have been reported, chemically and physically, to achieve such nanostructures. In a typical chemical preparation, n-alkyltrialkoxysilane or other surfactants are mixed with other precursors and are incorporated into the matrices during particle formation. These surfactants will be removed later from the nanostructure via post-synthesis solvent extraction or calcinations to yield the mesoporous structure. With the molecular-sieve structure, such mesoporous silica nanoparticles can load many small molecule pharmaceuticals via simple physical interaction. Furthermore, technologies have been developed to cap the mesopores after drug loading to inhibit premature drug release. For instance, mesoporous silica nanoparticles were loaded with PTX, and the mesopores were subsequently capped with Au NPs. Such Au NP capping was designed to be photolabile and can be uncapped to release guest molecules

when photoirradiated. Similarly, activatable gatekeepers based on QDs, IONPs, coumarin and diethylenetriamine have also been reported.

More recently, Park et al. reported on the preparation and application of luminescent porous silicon nanoparticles (LPSiNPs) (Fig. 7). The nanoparticles were made in physical ways. A typical preparation consisted of HF etching of single-crystal silicon wafers, lifting-off of the porous silicon film, ultrasonication, filtration of the formed particles through a 0.22 μm filtration membrane and finally activation of luminescence in an aqueous solution. The luminescence was generated by quantum confinement effects and the defects localized at the Si-SiO₂ interface. Such luminescent porous nanoparticles were loaded with DOX and their drug release and cytotoxicity were studied *in vitro*. One unique feature of such silica nanoparticles is that they can self-destruct *in vivo* and be renally cleared within a relatively short period of time, therefore reducing the risk of their getting trapped in and causing damage to normal organs.

7. Conclusions

In the current article, we have highlighted some nanoplatfoms that are currently under intensive investigation for the build-up of theranostic agents. All of the nanoplatfoms discussed here have gone through years of development and allow facile and reliable function docking. These nanoparticles can possess unique optical or magnetic properties and have been previously studied in the imaging setting and have achieved many successes. These have laid the foundation for the current exploits, since the imaging probes can be easily upgraded when loaded with appropriate therapeutics. It has been shown that therapeutics of various forms, including those that are small molecule, protein and nucleotide-based, can be conveniently tethered onto nanoplatfoms. The great capacity even allows the loading of a second or third functionality, a feature which encourages the formation of an all-in-one nanosystem with comprehensive features.

However, despite the fast progress, there has so far been no nanoparticle theranotics that is so developed to meet clinical standards. Each nanoplatfom has its own promises and advantages, but meanwhile, has its disadvantages to be overcome. These include the toxicity of QDs, the cost of gold nanoparticles, the intrinsic low sensitivity of IONP as MRI contrast probes, the nonbiodegradable nature of CNTs, and the oversize of silica nanoparticles, to name a few. Efforts to address each of these issues are going on, and should remain the focus in the future studies. Furthermore, as drug carriers, specific targeting is a topic that can never be over addressed. We have discussed the efforts of introducing a targeting motif onto nanoplatfoms to achieve an improved targeting profile. While this route should continue to be exploited, it is also advisable to address the issue by using nanoparticle-based hyperthermia, where treatment only occurs in a confined region and allows minimal normal tissue damage.

In addition to achieving and validating the nanoscale integration of imaging and therapeutic functions, it is of significant importance to demonstrate the benefits and synergy of such a combined approach. In theory, a NP-based theranostic agent can deliver therapeutics to a diseased area and can use its imaging function to improve diagnosis and to monitor therapeutic response. Despite the promise, the related proofs are so far inadequate and should be the main focus of the next stages of investigation.

Acknowledgments

This work was supported by the Intramural Research Program, NIBIB, NIH. S.L. is partially funded by the NIH/NIST NRC fellowship. We acknowledge Dr. Henry S. Eden for proofreading this manuscript.

References

1. Del Vecchio S, Zannetti A, Fonti R, Pace L, Salvatore M. Nuclear imaging in cancer theranostics. *Q J Nucl Med Mol Imaging*. 2007; 51:152–163. [PubMed: 17420716]
2. Nie S, Xing Y, Kim GJ, Simons JW. Nanotechnology applications in cancer. *Annu Rev Biomed Eng*. 2007; 9:257–288. [PubMed: 17439359]
3. Liu Y, Miyoshi H, Nakamura M. Nanomedicine for drug delivery and imaging: a promising avenue for cancer therapy and diagnosis using targeted functional nanoparticles. *Int J Cancer*. 2007; 120:2527–2537. [PubMed: 17390371]
4. Cai W, Chen X. Multimodality molecular imaging of tumor angiogenesis. *J Nucl Med*. 2008; 49(Suppl 2):113S–128S. [PubMed: 18523069]
5. Cai W, Chen X. Nanoplatforms for targeted molecular imaging in living subjects. *Small*. 2007; 3:1840–1854. [PubMed: 17943716]
6. Corot C, Robert P, Idee JM, Port M. Recent advances in iron oxide nanocrystal technology for medical imaging. *Adv Drug Deliv Rev*. 2006; 58:1471–1504. [PubMed: 17116343]
7. Park K, Lee S, Kang E, Kim K, Choi K, Kwon IC. New Generation of Multifunctional Nanoparticles for Cancer Imaging and Therapy. *Advanced Functional Materials*. 2009; 19:1553–1566.
8. Smith AM, Duan H, Mohs AM, Nie S. Bioconjugated quantum dots for in vivo molecular and cellular imaging. *Adv Drug Deliv Rev*. 2008; 60:1226–1240. [PubMed: 18495291]
9. Morales MP, Veintemillas-Verdaguer S, Montero MI, Serna CJ, Roig A, Casas L, Martinez B, Sandiumenge F. Surface and internal spin canting in gamma-Fe₂O₃ nanoparticles. *Chemistry of Materials*. 1999; 11:3058–3064.
10. Xie J, Huang J, Li X, Sun S, Chen X. Iron oxide nanoparticle platform for biomedical applications. *Curr Med Chem*. 2009; 16:1278–1294. [PubMed: 19355885]
11. Jun YW, Seo JW, Cheon A. Nanoscaling laws of magnetic nanoparticles and their applicabilities in biomedical sciences. *Accounts of Chemical Research*. 2008; 41:179–189. [PubMed: 18281944]
12. Xu CJ, Sun SH. Monodisperse magnetic nanoparticles for biomedical applications. *Polymer International*. 2007; 56:821–826.
13. Chouly C, Pouliquen D, Lucet I, Jeune JJ, Jallet P. Development of superparamagnetic nanoparticles for MRI: Effect of particle size, charge and surface nature on biodistribution. *J Microencapsul*. 1996; 13:245–255. [PubMed: 8860681]
14. Corot C, Violas X, Robert P, Gagneur G, Port M. Comparison of different types of blood pool agents (P792, MS325, USPIO) in a rabbit MR angiography-like protocol. *Invest Radiol*. 2003; 38:311–319. [PubMed: 12908698]
15. Duguet E, Vasseur S, Mornet S, Devoisselle JM. Magnetic nanoparticles and their applications in medicine. *Nanomedicine*. 2006; 1:157–168. [PubMed: 17716105]
16. Edelstein, AS.; Cammarata, RC. Institute of Physics (Great Britain). *Nanomaterials: synthesis, properties, and applications*. Institute of Physics Publishing; Bristol: 1996.
17. Fleige G, Seeberger F, Laux D, Kresse M, Taupitz M, Pilgrimm H, Zimmer C. In vitro characterization of two different ultrasmall iron oxide particles for magnetic resonance cell tracking. *Invest Radiol*. 2002; 37:482–488. [PubMed: 12218443]
18. Grancharov SG, Zeng H, Sun SH, Wang SX, O'Brien S, Murray CB, Kirtley JR, Held GA. Bio-functionalization of monodisperse magnetic nanoparticles and their use as biomolecular labels in a magnetic tunnel junction based sensor. *J Phys Chem B*. 2005; 109:13030–13035. [PubMed: 16852617]
19. Ito A, Shinkai M, Honda H, Kobayashi T. Medical application of functionalized magnetic nanoparticles. *J Biosci Bioeng*. 2005; 100:1–11. [PubMed: 16233845]
20. Lu AH, Salabas EL, Schuth F. Magnetic nanoparticles: Synthesis, protection, functionalization, and application. *Angew Chem Int Ed*. 2007; 46:1222–1244.
21. Kang YS, Risbud S, Rabolt JF, Stroeve P. Synthesis and characterization of nanometer-size Fe₃O₄ and gamma-Fe₂O₃ particles. *Chem Mater*. 1996; 8:2209–2211.
22. Gupta AK, Gupta M. Synthesis and surface engineering of iron oxide nanoparticles for biomedical applications. *Biomaterials*. 2005; 26:3995–4021. [PubMed: 15626447]

23. Lanza GM, Winter PM, Caruthers SD, Morawski AM, Schmieder AH, Crowder KC, Wickline SA. Magnetic resonance molecular imaging with nanoparticles. *J Nucl Cardiol*. 2004; 11:733–743. [PubMed: 15592197]
24. Mornet S, Vasseur S, Grasset F, Duguet E. Magnetic nanoparticle design for medical diagnosis and therapy. *J Mater Chem*. 2004; 14:2161–2175.
25. Harisinghani MG, Barentsz J, Hahn PF, Deserno WM, Tabatabaei S, van de Kaa CH, de la Rosette J, Weissleder R. Noninvasive detection of clinically occult lymph-node metastases in prostate cancer. *N Engl J Med*. 2003; 348:2491–2499. [PubMed: 12815134]
26. Lee HY, Li Z, Chen K, Hsu AR, Xu C, Xie J, Sun S, Chen X. PET/MRI dual-modality tumor imaging using arginine-glycine-aspartic (RGD)-conjugated radiolabeled iron oxide nanoparticles. *J Nucl Med*. 2008; 49:1371–1379. [PubMed: 18632815]
27. Pirko I, Johnson A, Ciric B, Gamez J, Macura SI, Pease LR, Rodriguez M. In vivo magnetic resonance imaging of immune cells in the central nervous system with superparamagnetic antibodies. *FASEB J*. 2003; 17:179–182. [PubMed: 14630708]
28. Zhao M, Kircher MF, Josephson L, Weissleder R. Differential conjugation of tat peptide to superparamagnetic nanoparticles and its effect on cellular uptake. *Bioconjug Chem*. 2002; 13:840–844. [PubMed: 12121140]
29. Kang HW, Josephson L, Petrovsky A, Weissleder R, Bogdanov A. Magnetic resonance imaging of inducible E-selectin expression in human endothelial cell culture. *Bioconjug Chem*. 2002; 13:122–127. [PubMed: 11792187]
30. Josephson L, Tung CH, Moore A, Weissleder R. High-efficiency intracellular magnetic labeling with novel superparamagnetic-tat peptide conjugates. *Bioconjug Chem*. 1999; 10:186–191. [PubMed: 10077466]
31. Hogemann D, Ntziachristos V, Josephson L, Weissleder R. High throughput magnetic resonance imaging for evaluating targeted nanoparticle probes. *Bioconjug Chem*. 2002; 13:116–121. [PubMed: 11792186]
32. Park J, Lee E, Hwang NM, Kang MS, Kim SC, Hwang Y, Park JG, Noh HJ, Kini JY, Park JH, Hyeon T. One-nanometer-scale size-controlled synthesis of monodisperse magnetic iron oxide nanoparticles. *Angew Chem Int Ed*. 2005; 44:2872–2877.
33. Kohler N, Fryxell GE, Zhang MQ. A bifunctional poly(ethylene glycol) silane immobilized on metallic oxide-based nanoparticles for conjugation with cell targeting agents. *Journal of the American Chemical Society*. 2004; 126:7206–7211. [PubMed: 15186157]
34. Kohler N, Sun C, Fichtenholtz A, Gunn J, Fang C, Zhang MQ. Methotrexate-immobilized poly(ethylene glycol) magnetic nanoparticles for MR imaging and drug delivery. *Small*. 2006; 2:785–792. [PubMed: 17193123]
35. Kohler N, Sun C, Wang J, Zhang MQ. Methotrexate-modified superparamagnetic nanoparticles and their intracellular uptake into human cancer cells. *Langmuir*. 2005; 21:8858–8864. [PubMed: 16142971]
36. Hwu JR, Lin YS, Josephraj T, Hsu MH, Cheng FY, Yeh CS, Su WC, Shieh DB. Targeted Paclitaxel by conjugation to iron oxide and gold nanoparticles. *J Am Chem Soc*. 2009; 131:66–68. [PubMed: 19072111]
37. Huh YM, Jun YW, Song HT, Kim S, Choi JS, Lee JH, Yoon S, Kim KS, Shin JS, Suh JS, Cheon J. In vivo magnetic resonance detection of cancer by using multifunctional magnetic nanocrystals. *J Am Chem Soc*. 2005; 127:12387–12391. [PubMed: 16131220]
38. Lee JH, Huh YM, Jun YW, Seo JW, Jang JT, Song HT, Kim S, Cho EJ, Yoon HG, Suh JS, Cheon J. Artificially engineered magnetic nanoparticles for ultra-sensitive molecular imaging. *Nat Med*. 2007; 13:95–99. [PubMed: 17187073]
39. Jain TK, Richey J, Strand M, Leslie-Pelecky DL, Flask CA, Labhasetwar V. Magnetic nanoparticles with dual functional properties: drug delivery and magnetic resonance imaging. *Biomaterials*. 2008; 29:4012–4021. [PubMed: 18649936]
40. Yu MK, Jeong YY, Park J, Park S, Kim JW, Min JJ, Kim K, Jon S. Drug-loaded superparamagnetic iron oxide nanoparticles for combined cancer imaging and therapy in vivo. *Angew Chem Int Ed Engl*. 2008; 47:5362–5365. [PubMed: 18551493]

41. Xie J, Chen K, Huang J, Lee S, Wang J, Gao J, Li X, Chen X. PET/NIRF/MRI triple functional iron oxide nanoparticles. *Biomaterials*. 31:3016–3022. [PubMed: 20092887]
42. Piao Y, Kim J, Bin Na H, Kim D, Baek JS, Ko MK, Lee JH, Shokouhimehr M, Hyeon T. Wrap-bake-peel process for nanostructural transformation from beta-FeOOH nanorods to biocompatible iron oxide nanocapsules. *Nature Materials*. 2008; 7:242–247.
43. Cheng K, Peng S, Xu C, Sun S. Porous hollow Fe(3)O(4) nanoparticles for targeted delivery and controlled release of cisplatin. *J Am Chem Soc*. 2009; 131:10637–10644. [PubMed: 19722635]
44. Medarova Z, Pham W, Farrar C, Petkova V, Moore A. In vivo imaging of siRNA delivery and silencing in tumors. *Nat Med*. 2007; 13:372–377. [PubMed: 17322898]
45. Lee JH, Lee K, Moon SH, Lee Y, Park TG, Cheon J. All-in-one target-cell-specific magnetic nanoparticles for simultaneous molecular imaging and siRNA delivery. *Angew Chem Int Ed Engl*. 2009; 48:4174–4179. [PubMed: 19408274]
46. Mornet S, Vasseur S, Grasset F, Duguet E. Magnetic nanoparticle design for medical diagnosis and therapy. *Journal of Materials Chemistry*. 2004; 14:2161–2175.
47. Ito A, Shinkai M, Honda H, Kobayashi T. Medical application of functionalized magnetic nanoparticles. *Journal of Bioscience and Bioengineering*. 2005; 100:1–11. [PubMed: 16233845]
48. Neuberger T, Schopf B, Hofmann H, Hofmann M, von Rechenberg B. Superparamagnetic nanoparticles for biomedical applications: Possibilities and limitations of a new drug delivery system. *Journal of Magnetism and Magnetic Materials*. 2005; 293:483–496.
49. Lubbe AS. Preclinical experiences with magnetic drug targeting: Tolerance and efficacy and clinical experiences with magnetic drug targeting: A phase I study with 4'-epidoxorubicin in 14 patients with advanced solid tumors - Reply. *Cancer Research*. 1997; 57:3064–3065.
50. Namiki Y, Namiki T, Yoshida H, Ishii Y, Tsubota A, Koido S, Nariai K, Mitsunaga M, Yanagisawa S, Kashiwagi H, Mabashi Y, Yumoto Y, Hoshina S, Fujise K, Tada N. A novel magnetic crystal-lipid nanostructure for magnetically guided in vivo gene delivery. *Nat Nanotechnol*. 2009; 4:598–606. [PubMed: 19734934]
51. Shinkai M, Le B, Honda H, Yoshikawa K, Shimizu K, Saga S, Wakabayashi T, Yoshida J, Kobayashi T. Targeting hyperthermia for renal cell carcinoma using human MN antigen-specific magnetoliposomes. *Japanese Journal of Cancer Research*. 2001; 92:1138–1145. [PubMed: 11676866]
52. Primo FL, Rodrigues MM, Simioni AR, Lacava ZG, Morais PC, Tedesco AC. Photosensitizer-loaded magnetic nanoemulsion for use in synergic photodynamic and magnetohyperthermia therapies of neoplastic cells. *J Nanosci Nanotechnol*. 2008; 8:5873–5877. [PubMed: 19198320]
53. Kim S, Lim YT, Soltész EG, De Grand AM, Lee J, Nakayama A, Parker JA, Mihaljevic T, Laurence RG, Dor DM, Cohn LH, Bawendi MG, Frangioni JV. Near-infrared fluorescent type II quantum dots for sentinel lymph node mapping. *Nat Biotechnol*. 2004; 22:93–97. [PubMed: 14661026]
54. Miao S, Hickey SG, Rellinghaus B, Waurisch C, Eychmuller A. Synthesis and characterization of cadmium phosphide quantum dots emitting in the visible red to near-infrared. *J Am Chem Soc*. 2006; 128:5613–5615. [PubMed: 20361738]
55. Zimmer JP, Kim SW, Ohnishi S, Tanaka E, Frangioni JV, Bawendi MG. Size series of small indium arsenide-zinc selenide core-shell nanocrystals and their application to in vivo imaging. *J Am Chem Soc*. 2006; 128:2526–2527. [PubMed: 16492023]
56. Xie R, Chen K, Chen X, Peng X. InAs/InP/ZnSe core/shell/shell quantum dots as near-infrared emitters: Bright, narrow-band, non-cadmium containing, and biocompatible. *Nano Res*. 2008; 1:457–464. [PubMed: 20631914]
57. Kim SW, Zimmer JP, Ohnishi S, Tracy JB, Frangioni JV, Bawendi MG. Engineering InAs(x)P(1-x)/InP/ZnSe III-V alloyed core/shell quantum dots for the near-infrared. *J Am Chem Soc*. 2005; 127:10526–10532. [PubMed: 16045339]
58. Bailey RE, Smith AM, Nie SM. Quantum dots in biology and medicine. *Physica E-Low-Dimensional Systems & Nanostructures*. 2004; 25:1–12.
59. Green M. Semiconductor quantum dots as biological imaging agents. *Angew Chem Int Ed Engl*. 2004; 43:4129–4131. [PubMed: 15307073]

60. Medintz IL, Uyeda HT, Goldman ER, Mattoussi H. Quantum dot bioconjugates for imaging, labelling and sensing. *Nat Mater.* 2005; 4:435–446. [PubMed: 15928695]
61. Choi HS, Liu W, Misra P, Tanaka E, Zimmer JP, Ipe BI, Bawendi MG, Frangioni JV. Renal clearance of quantum dots. *Nat Biotechnol.* 2007; 25:1165–1170. [PubMed: 17891134]
62. Kim S, Bawendi MG. Oligomeric ligands for luminescent and stable nanocrystal quantum dots. *J Am Chem Soc.* 2003; 125:14652–14653. [PubMed: 14640609]
63. Pinaud F, King D, Moore HP, Weiss S. Bioactivation and cell targeting of semiconductor CdSe/ZnS nanocrystals with phytochelatin-related peptides. *J Am Chem Soc.* 2004; 126:6115–6123. [PubMed: 15137777]
64. Smith AM, Nie S. Minimizing the hydrodynamic size of quantum dots with multifunctional multidentate polymer ligands. *J Am Chem Soc.* 2008; 130:11278–11279. [PubMed: 18680294]
65. Clapp AR, Medintz IL, Mauro JM, Fisher BR, Bawendi MG, Mattoussi H. Fluorescence resonance energy transfer between quantum dot donors and dye-labeled protein acceptors. *J Am Chem Soc.* 2004; 126:301–310. [PubMed: 14709096]
66. Medintz IL, Konnert JH, Clapp AR, Stanish I, Twigg ME, Mattoussi H, Mauro JM, Deschamps JR. A fluorescence resonance energy transfer-derived structure of a quantum dot-protein bioconjugate nanoassembly. *Proc Natl Acad Sci U S A.* 2004; 101:9612–9617. [PubMed: 15210939]
67. Carion O, Mahler B, Pons T, Dubertret B. Synthesis, encapsulation, purification and coupling of single quantum dots in phospholipid micelles for their use in cellular and in vivo imaging. *Nat Protoc.* 2007; 2:2383–2390. [PubMed: 17947980]
68. Dubertret B, Skourides P, Norris DJ, Noireaux V, Brivanlou AH, Libchaber A. In vivo imaging of quantum dots encapsulated in phospholipid micelles. *Science.* 2002; 298:1759–1762. [PubMed: 12459582]
69. Osaki F, Kanamori T, Sando S, Sera T, Aoyama Y. A quantum dot conjugated sugar ball and its cellular uptake. On the size effects of endocytosis in the subviral region. *J Am Chem Soc.* 2004; 126:6520–6521. [PubMed: 15161257]
70. Ballou B, Lagerholm BC, Ernst LA, Bruchez MP, Waggoner AS. Noninvasive imaging of quantum dots in mice. *Bioconjugate Chemistry.* 2004; 15:79–86. [PubMed: 14733586]
71. Mattheakis LC, Dias JM, Choi YJ, Gong J, Bruchez MP, Liu JQ, Wang E. Optical coding of mammalian cells using semiconductor quantum dots. *Analytical Biochemistry.* 2004; 327:200–208. [PubMed: 15051536]
72. Gao X, Cui Y, Levenson RM, Chung LW, Nie S. In vivo cancer targeting and imaging with semiconductor quantum dots. *Nat Biotechnol.* 2004; 22:969–976. [PubMed: 15258594]
73. Nurunnabi M, Cho KJ, Choi JS, Huh KM, Lee YK. Targeted near-IR QDs-loaded micelles for cancer therapy and imaging. *Biomaterials.*
74. Park JH, von Maltzahn G, Ruoslahti E, Bhatia SN, Sailor MJ. Micellar hybrid nanoparticles for simultaneous magnetofluorescent imaging and drug delivery. *Angew Chem Int Ed Engl.* 2008; 47:7284–7288. [PubMed: 18696519]
75. Bagalkot V, Zhang L, Levy-Nissenbaum E, Jon S, Kantoff PW, Langer R, Farokhzad OC. Quantum dot-aptamer conjugates for synchronous cancer imaging, therapy, and sensing of drug delivery based on bi-fluorescence resonance energy transfer. *Nano Lett.* 2007; 7:3065–3070. [PubMed: 17854227]
76. Yuan J, Guo W, Yang X, Wang E. Anticancer drug-DNA interactions measured using a photoinduced electron-transfer mechanism based on luminescent quantum dots. *Anal Chem.* 2009; 81:362–368. [PubMed: 19117462]
77. Chen AA, Derfus AM, Khetani SR, Bhatia SN. Quantum dots to monitor RNAi delivery and improve gene silencing. *Nucleic Acids Res.* 2005; 33:e190. [PubMed: 16352864]
78. Qi L, Gao X. Quantum dot-ampipol nanocomplex for intracellular delivery and real-time imaging of siRNA. *Acs Nano.* 2008; 2:1403–1410. [PubMed: 19206308]
79. Yezhelyev MV, Qi L, O'Regan RM, Nie S, Gao X. Proton-sponge coated quantum dots for siRNA delivery and intracellular imaging. *J Am Chem Soc.* 2008; 130:9006–9012. [PubMed: 18570415]
80. Derfus AM, Chen AA, Min DH, Ruoslahti E, Bhatia SN. Targeted quantum dot conjugates for siRNA delivery. *Bioconjug Chem.* 2007; 18:1391–1396. [PubMed: 17630789]

81. Bonoiu A, Mahajan SD, Ye L, Kumar R, Ding H, Yong KT, Roy I, Aalinkeel R, Nair B, Reynolds JL, Sykes DE, Imperiale MA, Bergey EJ, Schwartz SA, Prasad PN. MMP-9 gene silencing by a quantum dot-siRNA nanoplex delivery to maintain the integrity of the blood brain barrier. *Brain Res.* 2009; 1282:142–155. [PubMed: 19477169]
82. Samia AC, Chen X, Burda C. Semiconductor quantum dots for photodynamic therapy. *J Am Chem Soc.* 2003; 125:15736–15737. [PubMed: 14677951]
83. Willard DM, Van Orden A. Quantum dots: Resonant energy-transfer sensor. *Nat Mater.* 2003; 2:575–576. [PubMed: 12951597]
84. Bakalova R, Ohba H, Zhelev Z, Ishikawa M, Baba Y. Quantum dots as photosensitizers? *Nat Biotechnol.* 2004; 22:1360–1361. [PubMed: 15529155]
85. Tsay JM, Trzoss M, Shi L, Kong X, Selke M, Jung ME, Weiss S. Singlet oxygen production by Peptide-coated quantum dot-photosensitizer conjugates. *J Am Chem Soc.* 2007; 129:6865–6871. [PubMed: 17477530]
86. Samia AC, Dayal S, Burda C. Quantum dot-based energy transfer: perspectives and potential for applications in photodynamic therapy. *Photochem Photobiol.* 2006; 82:617–625. [PubMed: 16475871]
87. Hsieh JM, Ho ML, Wu PW, Chou PT, Tsai TT, Chi Y. Iridium-complex modified CdSe/ZnS quantum dots; a conceptual design for bi-functionality toward imaging and photosensitization. *Chem Commun (Camb).* 2006:615–617. [PubMed: 16446827]
88. Shi L, Hernandez B, Selke M. Singlet oxygen generation from water-soluble quantum dot-organic dye nanocomposites. *J Am Chem Soc.* 2006; 128:6278–6279. [PubMed: 16683767]
89. Daniel MC, Astruc D. Gold nanoparticles: Assembly, supramolecular chemistry, quantum-size-related properties, and applications toward biology, catalysis, and nanotechnology. *Chemical Reviews.* 2004; 104:293–346. [PubMed: 14719978]
90. Biju V, Itoh T, Anas A, Sujith A, Ishikawa M. Semiconductor quantum dots and metal nanoparticles: syntheses, optical properties, and biological applications. *Anal Bioanal Chem.* 2008; 391:2469–2495. [PubMed: 18548237]
91. Niemeyer CM. Nanoparticles, proteins, and nucleic acids: Biotechnology meets materials science. *Angewandte Chemie-International Edition.* 2001; 40:4128–4158.
92. Hu M, Chen JY, Li ZY, Au L, Hartland GV, Li XD, Marquez M, Xia YN. Gold nanostructures: engineering their plasmonic properties for biomedical applications. *Chemical Society Reviews.* 2006; 35:1084–1094. [PubMed: 17057837]
93. Murphy CJ, San TK, Gole AM, Orendorff CJ, Gao JX, Gou L, Hunyadi SE, Li T. Anisotropic metal nanoparticles: Synthesis, assembly, and optical applications. *Journal of Physical Chemistry B.* 2005; 109:13857–13870.
94. Murphy CJ, Sau TK, Gole A, Orendorff CJ. Surfactant-directed synthesis and optical properties of one-dimensional plasmonic metallic nanostructures. *Mrs Bulletin.* 2005; 30:349–355.
95. Chen J, Saeki F, Wiley BJ, Cang H, Cobb MJ, Li ZY, Au L, Zhang H, Kimmey MB, Li XD, Xia Y. Gold nanocages: Bioconjugation and their potential use as optical imaging contrast agents. *Nano Lett.* 2005; 5:473–477. [PubMed: 15755097]
96. Wang C, Hu Y, Lieber CM, Sun S. Ultrathin Au nanowires and their transport properties. *J Am Chem Soc.* 2008; 130:8902–8903. [PubMed: 18540579]
97. Link S, El-Sayed MA. Size and temperature dependence of the plasmon absorption of colloidal gold nanoparticles. *Journal of Physical Chemistry B.* 1999; 103:4212–4217.
98. Murphy CJ, Sau TK, Gole AM, Orendorff CJ, Gao J, Gou L, Hunyadi SE, Li T. Anisotropic metal nanoparticles: Synthesis, assembly, and optical applications. *J Phys Chem B.* 2005; 109:13857–13870. [PubMed: 16852739]
99. Dixit V, Van den Bossche J, Sherman DM, Thompson DH, Andres RP. Synthesis and grafting of thioctic acid-PEG-folate conjugates onto Au nanoparticles for selective targeting of folate receptor-positive tumor cells. *Bioconjugate Chemistry.* 2006; 17:603–609. [PubMed: 16704197]
100. Oyelere AK, Chen PC, Huang X, El-Sayed IH, El-Sayed MA. Peptide-conjugated gold nanorods for nuclear targeting. *Bioconjug Chem.* 2007; 18:1490–1497. [PubMed: 17630680]

101. Reynolds AJ, Haines AH, Russell DA. Gold glyconanoparticles for mimics and measurement of metal ion-mediated carbohydrate-carbohydrate interactions. *Langmuir*. 2006; 22:1156–1163. [PubMed: 16430279]
102. Rosi NL, Giljohann DA, Thaxton CS, Lytton-Jean AK, Han MS, Mirkin CA. Oligonucleotide-modified gold nanoparticles for intracellular gene regulation. *Science*. 2006; 312:1027–1030. [PubMed: 16709779]
103. Chang JY, Wu HM, Chen H, Ling YC, Tan WH. Oriented assembly of Au nanorods using biorecognition system. *Chemical Communications*. 2005:1092–1094. [PubMed: 15719127]
104. Huang XH, El-Sayed IH, Qian W, El-Sayed MA. Cancer cells assemble and align gold nanorods conjugated to antibodies to produce highly enhanced, sharp, and polarized surface Raman spectra: A potential cancer diagnostic marker. *Nano Lett*. 2007; 7:1591–1597. [PubMed: 17474783]
105. Gibson JD, Khanal BP, Zubarev ER. Paclitaxel-functionalized gold nanoparticles. *J Am Chem Soc*. 2007; 129:11653–11661. [PubMed: 17718495]
106. Chen YH, Tsai CY, Huang PY, Chang MY, Cheng PC, Chou CH, Chen DH, Wang CR, Shiau AL, Wu CL. Methotrexate conjugated to gold nanoparticles inhibits tumor growth in a syngeneic lung tumor model. *Mol Pharm*. 2007; 4:713–722. [PubMed: 17708653]
107. Paciotti GF, Myer L, Weinreich D, Goia D, Pavel N, McLaughlin RE, Tamarkin L. Colloidal gold: a novel nanoparticle vector for tumor directed drug delivery. *Drug Deliv*. 2004; 11:169–183. [PubMed: 15204636]
108. Goel R, Shah N, Visaria R, Paciotti GF, Bischof JC. Biodistribution of TNF-alpha-coated gold nanoparticles in an in vivo model system. *Nanomedicine (Lond)*. 2009; 4:401–410. [PubMed: 19505243]
109. Powell AC, Paciotti GF, Libutti SK. Colloidal gold: a novel nanoparticle for targeted cancer therapeutics. *Methods Mol Biol*. 624:375–384. [PubMed: 20217609]
110. Bhumkar DR, Joshi HM, Sastry M, Pokharkar VB. Chitosan reduced gold nanoparticles as novel carriers for transmucosal delivery of insulin. *Pharm Res*. 2007; 24:1415–1426. [PubMed: 17380266]
111. Cheng Y, Meyers CSAJD, Panagopoulos I, Fei B, Burda C. Highly efficient drug delivery with gold nanoparticle vectors for in vivo photodynamic therapy of cancer. *J Am Chem Soc*. 2008; 130:10643–10647. [PubMed: 18642918]
112. Hone DC, Walker PI, Evans-Gowing R, FitzGerald S, Beeby A, Chambrier I, Cook MJ, Russell DA. Generation of cytotoxic singlet oxygen via phthalocyanine-stabilized gold nanoparticles: A potential delivery vehicle for photodynamic therapy. *Langmuir*. 2002; 18:2985–2987.
113. Prabakaran M, Grailer JJ, Pilla S, Steeber DA, Gong S. Gold nanoparticles with a monolayer of doxorubicin-conjugated amphiphilic block copolymer for tumor-targeted drug delivery. *Biomaterials*. 2009; 30:6065–6075. [PubMed: 19674777]
114. McIntosh CM, Esposito EA 3rd, Boal AK, Simard JM, Martin CT, Rotello VM. Inhibition of DNA transcription using cationic mixed monolayer protected gold clusters. *J Am Chem Soc*. 2001; 123:7626–7629. [PubMed: 11480984]
115. Han G, Martin CT, Rotello VM. Stability of gold nanoparticle-bound DNA toward biological, physical, and chemical agents. *Chem Biol Drug Des*. 2006; 67:78–82. [PubMed: 16492152]
116. Han G, Chari NS, Verma A, Hong R, Martin CT, Rotello VM. Controlled recovery of the transcription of nanoparticle-bound DNA by intracellular concentrations of glutathione. *Bioconjug Chem*. 2005; 16:1356–1359. [PubMed: 16287230]
117. Thomas M, Klibanov AM. Conjugation to gold nanoparticles enhances polyethylenimine's transfer of plasmid DNA into mammalian cells. *Proc Natl Acad Sci U S A*. 2003; 100:9138–9143. [PubMed: 12886020]
118. Huang X, El-Sayed IH, Qian W, El-Sayed MA. Cancer cells assemble and align gold nanorods conjugated to antibodies to produce highly enhanced, sharp, and polarized surface Raman spectra: a potential cancer diagnostic marker. *Nano Lett*. 2007; 7:1591–1597. [PubMed: 17474783]
119. Skrabalak SE, Chen J, Sun Y, Lu X, Au L, Cogley CM, Xia Y. Gold nanocages: synthesis, properties, and applications. *Acc Chem Res*. 2008; 41:1587–1595. [PubMed: 18570442]

120. Ji X, Shao R, Elliott AM, Stafford RJ, Esparza-Coss E, Liang G, Luo ZP, Park K, Markert JT, Li C. Bifunctional Gold Nanoshells with a Superparamagnetic Iron Oxide-Silica Core Suitable for Both MR Imaging and Photothermal Therapy. *J Phys Chem C Nanomater Interfaces*. 2007; 111:6245. [PubMed: 20165552]
121. Chen J, Glaus C, Laforest R, Zhang Q, Yang M, Gidding M, Welch MJ, Xia Y. Gold nanocages as photothermal transducers for cancer treatment. *Small*. 6:811–817. [PubMed: 20225187]
122. Lu W, Xiong C, Zhang G, Huang Q, Zhang R, Zhang JZ, Li C. Targeted photothermal ablation of murine melanomas with melanocyte-stimulating hormone analog-conjugated hollow gold nanospheres. *Clin Cancer Res*. 2009; 15:876–886. [PubMed: 19188158]
123. Lu W, Zhang G, Zhang R, Flores LG 2nd, Huang Q, Gelovani JG, Li C. Tumor site-specific silencing of NF-kappaB p65 by targeted hollow gold nanosphere-mediated photothermal transfection. *Cancer Res*. 70:3177–3188. [PubMed: 20388791]
124. Welsher K, Liu Z, Dai DDH. Selective Probing and Imaging of Cells with Single Walled Carbon Nanotubes as Near-Infrared Fluorescent Molecules. *Nano Lett*. 2008; 8:586–590. [PubMed: 18197719]
125. Liu Z, Li X, Tabakman SM, Jiang K, Fan S, Dai H. Multiplexed multi-color Raman imaging of live cells with isotopically modified single walled carbon nanotubes. *J Am Chem Soc*. 2008; 130:13540–13541. [PubMed: 18803379]
126. Kam NWS, O'Connell M, Wisdom JA, Dai H. Carbon nanotubes as multifunctional biological transporters and near-infrared agents for selective cancer cell destruction. *Proc Natl Acad Sci USA*. 2005; 102:11600–11605. [PubMed: 16087878]
127. Liu J, Rinzler AG, Dai H, Hafner JH, Bradley RK, Boul PJ, Lu A, Iverson T, Shelimov K, Huffman CB, Rodriguez-Macias F, Shon YS, Lee TR, Colbert DT, Smalley RE. Fullerene pipes. *Science*. 1998; 280:1253–1256. [PubMed: 9596576]
128. Shi Kam NW, Jessop TC, Wender PA, Dai H. Nanotube molecular transporters: internalization of carbon nanotube-protein conjugates into Mammalian cells. *J Am Chem Soc*. 2004; 126:6850–6851. [PubMed: 15174838]
129. Jiang KY, Schadler LS, Siegel RW, Zhang XJ, Zhang HF, Terrones M. Protein immobilization on carbon nanotubes via a two-step process of diimide-activated amidation. *Journal of Materials Chemistry*. 2004; 14:37–39.
130. Baker SE, Cai W, Lasseter TL, Weidkamp KP, Hamers RJ. Covalently bonded adducts of deoxyribonucleic acid (DNA) oligonucleotides with single-wall carbon nanotubes: Synthesis and hybridization. *Nano Lett*. 2002; 2:1413–1417.
131. Huang WJ, Taylor S, Fu KF, Lin Y, Zhang DH, Hanks TW, Rao AM, Sun YP. Attaching proteins to carbon nanotubes via diimide-activated amidation. *Nano Lett*. 2002; 2:311–314.
132. Pompeo F, Resasco DE. Water solubilization of single-walled carbon nanotubes by functionalization with glucosamine. *Nano Lett*. 2002; 2:369–373.
133. Peng H, Alemany LB, Margrave JL, Khabashesku VN. Sidewall carboxylic acid functionalization of single-walled carbon nanotubes. *J Am Chem Soc*. 2003; 125:15174–15182. [PubMed: 14653752]
134. Nguyen CV, Delzeit L, Cassell AM, Li J, Han J, Meyyappan M. Preparation of nucleic acid functionalized carbon nanotube Arrays. *Nano Lett*. 2002; 2:1079–1081.
135. Katz E, Willner I. Biomolecule-functionalized carbon nanotubes: applications in nanobioelectronics. *Chemphyschem*. 2004; 5:1084–1104. [PubMed: 15446731]
136. Bianco A, Kostarelos K, Partidos CD, Prato M. Biomedical applications of functionalised carbon nanotubes. *Chem Commun (Camb)*. 2005:571–577. [PubMed: 15672140]
137. Islam MF, Rojas E, Bergy DM, Johnson AT, Yodh AG. High weight fraction surfactant solubilization of single-wall carbon nanotubes in water. *Nano Lett*. 2003; 3:269–273.
138. Nakashima N, Tomonari Y, Murakami H. Water-soluble single-walled carbon nanotubes via noncovalent sidewall-functionalization with a pyrene-carrying ammonium ion. *Chemistry Letters*. 2002:638–639.
139. Moore VC, Strano MS, Haroz EH, Hauge RH, Smalley RE, Schmidt J, Talmon Y. Individually suspended single-walled carbon nanotubes in various surfactants. *Nano Lett*. 2003; 3:1379–1382.

140. Chen RJ, Zhang YG, Wang DW, Dai HJ. Noncovalent sidewall functionalization of single-walled carbon nanotubes for protein immobilization. *J Am Chem Soc.* 2001; 123:3838–3839. [PubMed: 11457124]
141. Kang Y, Taton TA. Micelle-encapsulated carbon nanotubes: a route to nanotube composites. *J Am Chem Soc.* 2003; 125:5650–5651. [PubMed: 12733901]
142. Artyukhin AB, Bakajin O, Stroeve P, Noy A. Layer-by-layer electrostatic self-assembly of polyelectrolyte nanoshells on individual carbon nanotube templates. *Langmuir.* 2004; 20:1442–1448. [PubMed: 15803732]
143. Zheng M, Jagota A, Semke ED, Diner BA, Mclean RS, Lustig SR, Richardson RE, Tassi NG. DNA-assisted dispersion and separation of carbon nanotubes. *Nature Materials.* 2003; 2:338–342.
144. Zheng M, Jagota A, Strano MS, Santos AP, Barone P, Chou SG, Diner BA, Dresselhaus MS, McLean RS, Onoa GB, Samsonidze GG, Semke ED, Usrey M, Walls DJ. Structure-based carbon nanotube sorting by sequence-dependent DNA assembly. *Science.* 2003; 302:1545–1548. [PubMed: 14645843]
145. Johnson RR, Johnson ATC, Klein ML. Probing the structure of DNA-carbon nanotube hybrids with molecular dynamics. *Nano Lett.* 2008; 8:69–75. [PubMed: 18069867]
146. Schipper ML, Nakayama-Ratchford N, Davis CR, Kam NWS, Chu P, Liu Z, Sun XM, Dai HJ, Gambhir SS. A pilot toxicology study of single-walled carbon nanotubes in a small sample of mice. *Nature Nanotechnology.* 2008; 3:216–221.
147. Kam NW, Liu Z, Dai H. Carbon nanotubes as intracellular transporters for proteins and DNA: an investigation of the uptake mechanism and pathway. *Angew Chem Int Ed Engl.* 2006; 45:577–581. [PubMed: 16345107]
148. Jin H, Heller DA, Strano MS. Single-particle tracking of endocytosis and exocytosis of single-walled carbon nanotubes in NIH-3T3 cells. *Nano Lett.* 2008; 8:1577–1585. [PubMed: 18491944]
149. Kostarelos K, Lacerda L, Pastorin G, Wu W, Wieckowski S, Luangsivilay J, Godefroy S, Pantarotto D, Briand JP, Muller S, Prato M, Bianco A. Cellular uptake of functionalized carbon nanotubes is independent of functional group and cell type. *Nat Nanotechnol.* 2007; 2:108–113. [PubMed: 18654229]
150. Pantarotto D, Singh R, McCarthy D, Erhardt M, Briand JP, Prato M, Kostarelos K, Bianco A. Functionalized carbon nanotubes for plasmid DNA gene delivery. *Angew Chem Int Ed Engl.* 2004; 43:5242–5246. [PubMed: 15455428]
151. Singh R, Pantarotto D, McCarthy D, Chaloin O, Hoebeke J, Partidos CD, Briand JP, Prato M, Bianco A, Kostarelos K. Binding and condensation of plasmid DNA onto functionalized carbon nanotubes: toward the construction of nanotube-based gene delivery vectors. *J Am Chem Soc.* 2005; 127:4388–4396. [PubMed: 15783221]
152. Pastorin G, Wu W, Wieckowski S, Briand JP, Kostarelos K, Prato M, Bianco A. Double functionalization of carbon nanotubes for multimodal drug delivery. *Chem Commun (Camb).* 2006:1182–1184. [PubMed: 16518484]
153. Kam NW, Liu Z, Dai H. Functionalization of carbon nanotubes via cleavable disulfide bonds for efficient intracellular delivery of siRNA and potent gene silencing. *J Am Chem Soc.* 2005; 127:12492–12493. [PubMed: 16144388]
154. Liu Z, Winters M, Holodniy M, Dai H. siRNA delivery into human T cells and primary cells with carbon-nanotube transporters. *Angew Chem Int Ed Engl.* 2007; 46:2023–2027. [PubMed: 17290476]
155. Dhar S, Liu Z, Thomale J, Dai H, Lippard SJ. Targeted single-wall carbon nanotube-mediated Pt(IV) prodrug delivery using folate as a homing device. *J Am Chem Soc.* 2008; 130:11467–11476. [PubMed: 18661990]
156. Liu Z, Chen K, Davis C, Sherlock S, Cao Q, Chen X, Dai H. Drug delivery with carbon nanotubes for in vivo cancer treatment. *Cancer Res.* 2008; 68:6652–6660. [PubMed: 18701489]
157. Liu Z, Tabakman S, Welsher K, Dai H. Carbon Nanotubes in Biology and Medicine: In vitro and in vivo Detection, Imaging and Drug Delivery. *Nano Res.* 2009; 2:85–120. [PubMed: 20174481]

158. Liu Z, Fan AC, Rakhra K, Sherlock S, Goodwin A, Chen X, Yang Q, Felsher DW, Dai H. Supramolecular stacking of doxorubicin on carbon nanotubes for in vivo cancer therapy. *Angew Chem Int Ed Engl.* 2009; 48:7668–7672. [PubMed: 19760685]
159. Kam NW, O'Connell M, Wisdom JA, Dai H. Carbon nanotubes as multifunctional biological transporters and near-infrared agents for selective cancer cell destruction. *Proc Natl Acad Sci U S A.* 2005; 102:11600–11605. [PubMed: 16087878]
160. Moon HK, Lee SH, Choi HC. In vivo near-infrared mediated tumor destruction by photothermal effect of carbon nanotubes. *ACS Nano.* 2009; 3:3707–3713. [PubMed: 19877694]
161. Ghosh S, Dutta S, Gomes E, Carroll D, D'Agostino R Jr, Olson J, Guthold M, Gmeiner WH. Increased heating efficiency and selective thermal ablation of malignant tissue with DNA-encased multiwalled carbon nanotubes. *ACS Nano.* 2009; 3:2667–2673. [PubMed: 19655728]
162. Jana NR, Earhart C, Ying JY. Synthesis of water-soluble and functionalized nanoparticles by silica coating. *Chem Mater.* 2007; 19:5074–5082.
163. Ow H, Larson DR, Srivastava M, Baird BA, Webb WW, Wiesner U. Bright and stable core-shell fluorescent silica nanoparticles. *Nano Lett.* 2005; 5:113–117. [PubMed: 15792423]
164. Tapeç R, Zhao XJ, Tan W. Development of organic dye-doped silica nanoparticles for bioanalysis and biosensors. *J Nanosci Nanotechnol.* 2002; 2:405–409. [PubMed: 12908270]
165. Hsiao JK, Tsai CP, Chung TH, Hung Y, Yao M, Liu HM, Mou CY, Yang CS, Chen YC, Huang DM. Mesoporous silica nanoparticles as a delivery system of gadolinium for effective human stem cell tracking. *Small.* 2008; 4:1445–1452. [PubMed: 18680095]
166. Wolcott A, Gerion D, Visconte M, Sun J, Schwartzberg A, Chen SW, Zhang JZ. Silica-coated CdTe quantum dots functionalized with thiols for bioconjugation to IgG proteins. *Journal of Physical Chemistry B.* 2006; 110:5779–5789.
167. Gerion D, Pinaud F, Williams SC, Parak WJ, Zanchet D, Weiss S, Alivisatos AP. Synthesis and properties of biocompatible water-soluble silica-coated CdSe/ZnS semiconductor quantum dots. *Journal of Physical Chemistry B.* 2001; 105:8861–8871.
168. Kang K, Choi J, Nam JH, Lee SC, Kim KJ, Lee SW, Chang JH. Preparation and characterization of chemically functionalized silica-coated magnetic nanoparticles as a DNA separator. *J Phys Chem B.* 2009; 113:536–543. [PubMed: 19099431]
169. Wang CG, Chen Y, Wang TT, Ma ZF, Su ZM. Monodispersed gold nanorod-embedded silica particles as novel Raman labels for biosensing. *Advanced Functional Materials.* 2008; 18:355–361.
170. Lu CW, Hung Y, Hsiao JK, Yao M, Chung TH, Lin YS, Wu SH, Hsu SC, Liu HM, Mou CY, Yang CS, Huang DM, Chen YC. Bifunctional magnetic silica nanoparticles for highly efficient human stem cell labeling. *Nano Lett.* 2007; 7:149–154. [PubMed: 17212455]
171. Kim J, Lee JE, Lee J, Yu JH, Kim BC, An K, Hwang Y, Shin CH, Park JG, Hyeon T. Magnetic fluorescent delivery vehicle using uniform mesoporous silica spheres embedded with monodisperse magnetic and semiconductor nanocrystals. *J Am Chem Soc.* 2006; 128:688–689. [PubMed: 16417336]
172. Rieter WJ, Kim JS, Taylor KM, An H, Lin W, Tarrant T. Hybrid silica nanoparticles for multimodal imaging. *Angew Chem Int Ed Engl.* 2007; 46:3680–3682. [PubMed: 17415734]
173. Salgueirino-Maceira V, Correa-Duarte MA, Spasova M, Liz-Marzan LM, Farle M. Composite silica spheres with magnetic and luminescent functionalities. *Advanced Functional Materials.* 2006; 16:509–514.
174. Sathe TR, Agrawal A, Nie S. Mesoporous silica beads embedded with semiconductor quantum dots and iron oxide nanocrystals: dual-function microcarriers for optical encoding and magnetic separation. *Anal Chem.* 2006; 78:5627–5632. [PubMed: 16906704]
175. Selvan ST, Patra PK, Ang CY, Ying JY. Synthesis of silica-coated semiconductor and magnetic quantum dots and their use in the imaging of live cells. *Angew Chem Int Ed Engl.* 2007; 46:2448–2452. [PubMed: 17318931]
176. Yi DK, Selvan ST, Lee SS, Papaefthymiou GC, Kundaliya D, Ying JY. Silica-coated nanocomposites of magnetic nanoparticles and quantum dots. *J Am Chem Soc.* 2005; 127:4990–4991. [PubMed: 15810812]

177. Koole R, van Schooneveld MM, Hilhorst J, Castermans K, Cormode DP, Strijkers GJ, de Mello Donega C, Vanmaekelbergh D, Griffioen AW, Nicolay K, Fayad ZA, Meijerink A, Mulder WJ. Paramagnetic lipid-coated silica nanoparticles with a fluorescent quantum dot core: a new contrast agent platform for multimodality imaging. *Bioconjug Chem*. 2008; 19:2471–2479. [PubMed: 19035793]
178. Roy I, Ohulchanskyy TY, Pudavar HE, Bergey EJ, Oseroff AR, Morgan J, Dougherty TJ, Prasad PN. Ceramic-based nanoparticles entrapping water-insoluble photosensitizing anticancer drugs: a novel drug-carrier system for photodynamic therapy. *J Am Chem Soc*. 2003; 125:7860–7865. [PubMed: 12823004]
179. Kim S, Ohulchanskyy TY, Pudavar HE, Pandey RK, Prasad PN. Organically modified silica nanoparticles co-encapsulating photosensitizing drug and aggregation-enhanced two-photon absorbing fluorescent dye aggregates for two-photon photodynamic therapy. *J Am Chem Soc*. 2007; 129:2669–2675. [PubMed: 17288423]
180. Slowing II, Vivero-Escoto JL, Wu CW, Lin VS. Mesoporous silica nanoparticles as controlled release drug delivery and gene transfection carriers. *Adv Drug Deliv Rev*. 2008; 60:1278–1288. [PubMed: 18514969]
181. Vallet-Regi M, Balas F, Arcos D. Mesoporous materials for drug delivery. *Angew Chem Int Ed Engl*. 2007; 46:7548–7558. [PubMed: 17854012]
182. Manzano M, Colilla M, Vallet-Regi M. Drug delivery from ordered mesoporous matrices. *Expert Opin Drug Deliv*. 2009; 6:1383–1400. [PubMed: 19941412]
183. Vivero-Escoto JL, Slowing II, Wu CW, Lin VS. Photoinduced intracellular controlled release drug delivery in human cells by gold-capped mesoporous silica nanosphere. *J Am Chem Soc*. 2009; 131:3462–3463. [PubMed: 19275256]
184. Lai CY, Trewyn BG, Jęftinija DM, Jęftinija K, Xu S, Jęftinija S, Lin VS. A mesoporous silica nanosphere-based carrier system with chemically removable CdS nanoparticle caps for stimuli-responsive controlled release of neurotransmitters and drug molecules. *J Am Chem Soc*. 2003; 125:4451–4459. [PubMed: 12683815]
185. Giri S, Trewyn BG, Stellmaker MP, Lin VS. Stimuli-responsive controlled-release delivery system based on mesoporous silica nanorods capped with magnetic nanoparticles. *Angew Chem Int Ed Engl*. 2005; 44:5038–5044. [PubMed: 16038000]
186. Mal NK, Fujiwara M, Tanaka Y. Photocontrolled reversible release of guest molecules from coumarin-modified mesoporous silica. *Nature*. 2003; 421:350–353. [PubMed: 12540896]
187. Casasus R, Marcos MD, Martinez-Manez R, Ros-Lis JV, Soto J, Villaescusa LA, Amoros P, Beltran D, Guillem C, Latorre J. Toward the development of ionically controlled nanoscopic molecular gates. *J Am Chem Soc*. 2004; 126:8612–8613. [PubMed: 15250688]
188. Park JH, Gu L, von Maltzahn G, Ruoslahti E, Bhatia SN, Sailor MJ. Biodegradable luminescent porous silicon nanoparticles for in vivo applications. *Nat Mater*. 2009; 8:331–336. [PubMed: 19234444]

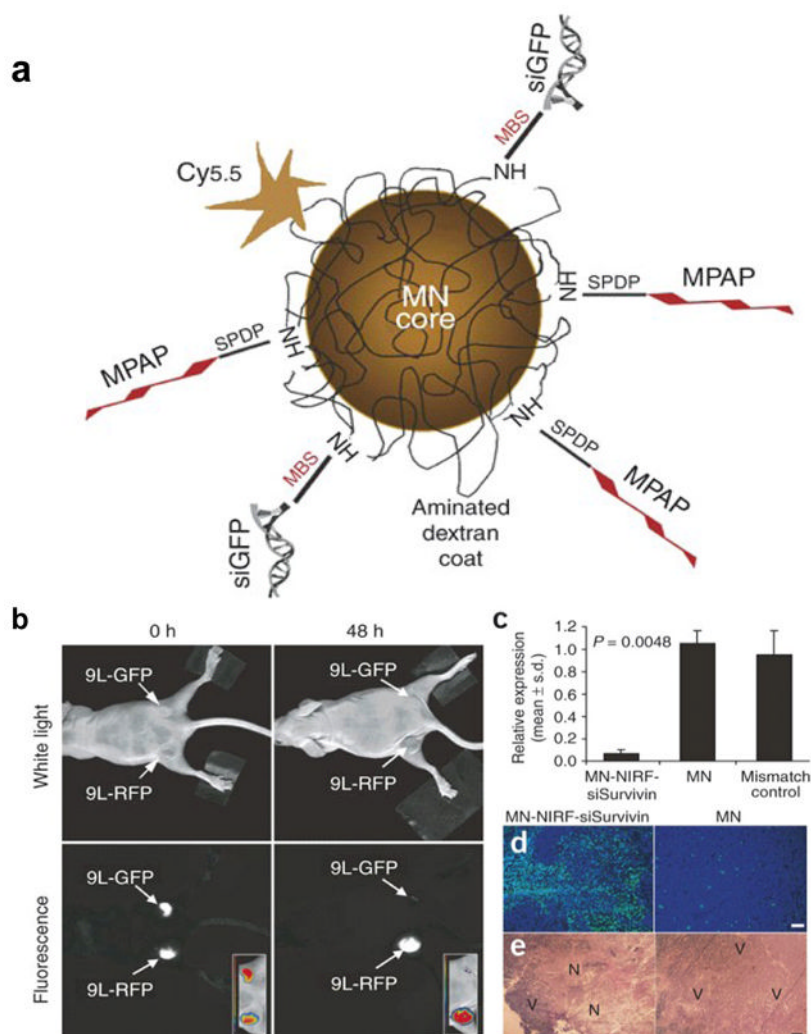


Fig. 1. (a) Illustrative demonstration of the formation of the siRNA-IONP nanoconjugate, which consists of magnetic nanoparticles labeled with near-infrared (NIRF) dye Cy5.5 and coupled with membrane translocation peptides (MPAP), and siRNA targeting GFP (switched to Survivin targeted siRNA in c, d, e). (b) *In vivo* NIRF optical imaging of mice bearing bilateral 9L-GFP and 9L-RFP tumors 48 h after intravenous probe injection. There was a marked decrease in 9L-GFP-associated fluorescence and no change in 9L-RFP fluorescence. (c-e) *Ex vivo* assays on tumor samples after siSurvivin-IONP conjugate treatment. (c) Quantitative RT-PCR analysis of survivin expression in LS174T tumors after mice were injected with either MN-NIRF-siSurvivin, a mismatch control, or the parent magnetic nanoparticle alone (MN). (d) Areas of high density apoptotic nuclei (green) were found in tumors treated with MN-NIRF-siSurvivin (left), but not in controls that received only parent magnetic nanoparticles (right). (e) H&E staining of frozen tumor sections revealed considerable eosinophilic areas of tumor necrosis (N) in tumors treated with MN-NIRF-siSurvivin (left). Tumors treated with magnetic nanoparticles were devoid of necrotic tissue (right). Purple hematoxiphilic regions (V) indicate viable tumor tissues. Scale bar, 50 μ m. Reprinted with permission from ref [44].

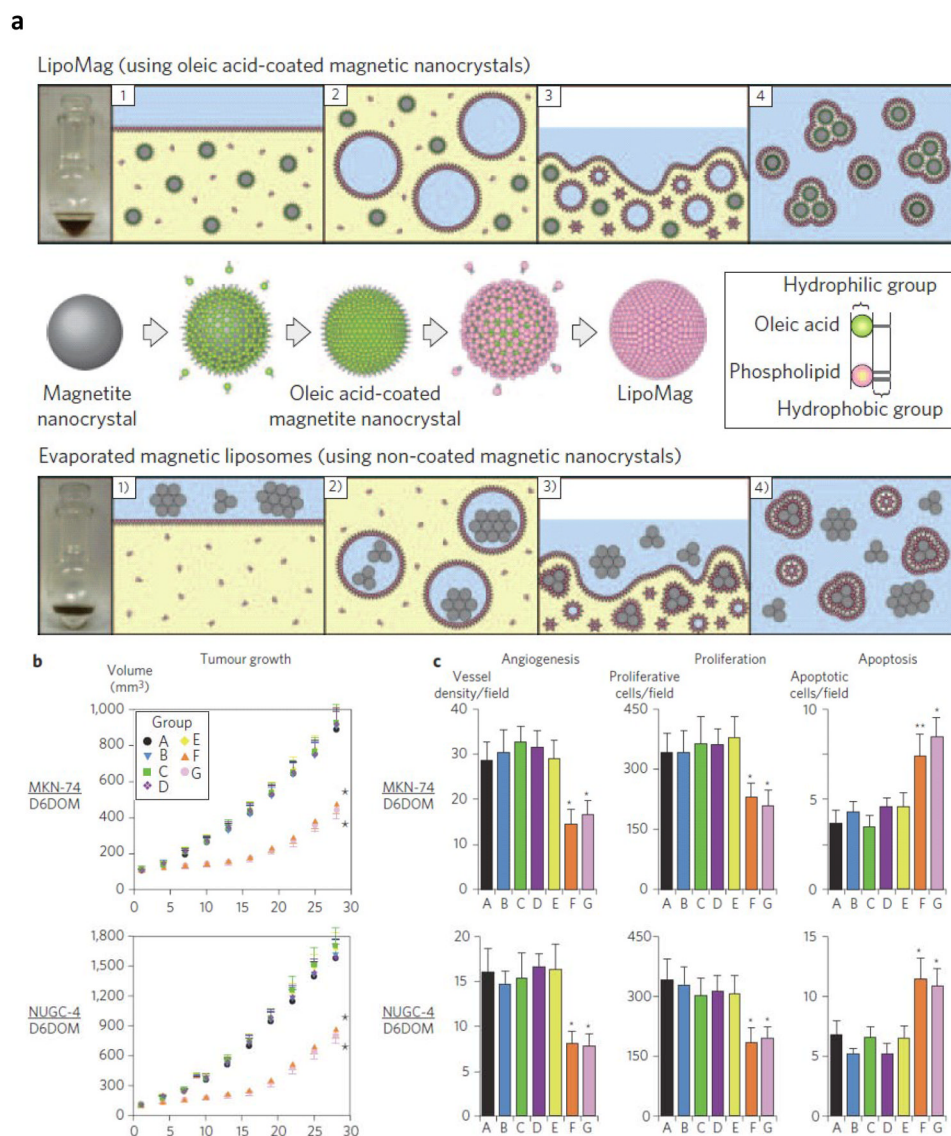


Fig. 2. (a) Schematic illustration of the preparation (upper) and assembly (middle) of LipoMag and reverse-phase evaporated magnetic liposomes (lower). (b-c) MKN-74- and NUGC-4-inoculated mice were given LipoMag-siRNA at 0, 2, 4, 6, 8, 10, 12 and 14 days after the initiation of treatment. The treatment schedule was as follows: Group A = control. Group B, C, D were injected with LipoMag loaded with control siRNA sequence. And among them, B was treated without magnetic field. C and D were treated with internal and external magnetic fields, respectively. Group E, F, G were given LipoMag loaded with the modified siRNA-EGFR#4 sequence. E was given the therapeutics without magnetic filed. F and G were injected with nanoparticle therapeutics with internal and external magnetic fields, respectively. (b) Tumor growth curve for each treatment over time. Only the LipoMag/siRNAEGFR groups under a magnetic field showed a significant anti-tumor effect. (c) Two days after the last treatment, the degree of angiogenesis, proliferation and apoptosis were assayed by immunostaining of vWF, Ki-67 and ssDNA, respectively. Reprinted with permission from ref [50].

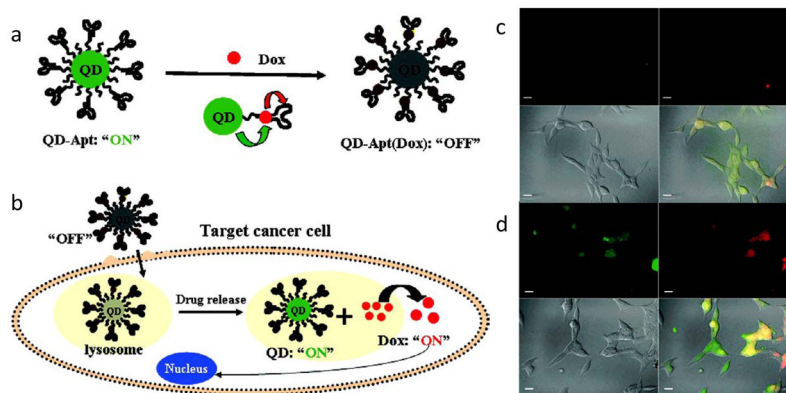
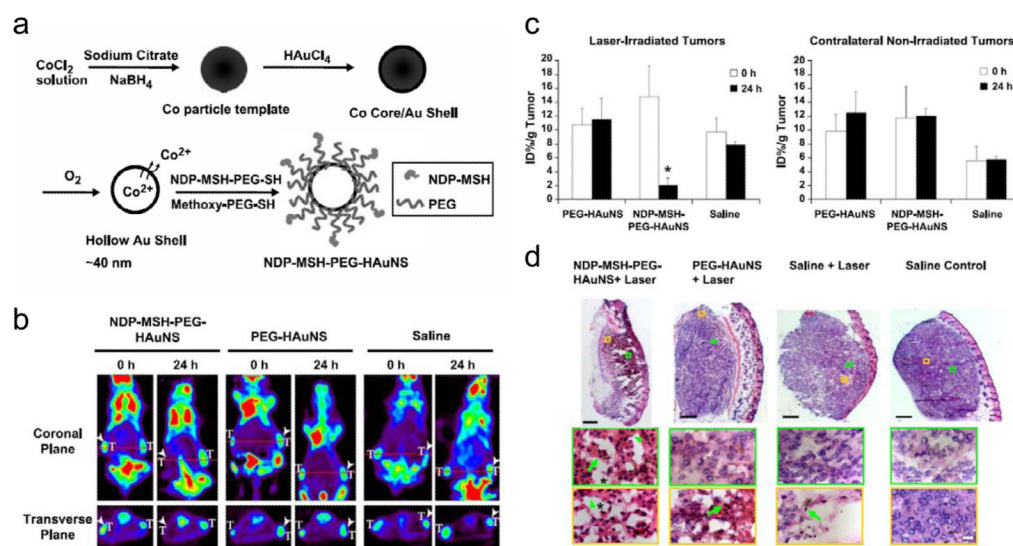


Fig. 3. (a) & (b) Formation and working mechanism of QD-Apt(Dox)-FRET nanosystem. (a) CdSe/ZnS QDs are surface functionalized with the A10 PSMA aptamer. The intercalation of Dox within the A10 PSMA aptamer on the surface of QDs resulted in the formation of the QD-Apt(Dox), which quenched fluorescence from both QD and Dox ("OFF" state). (b) Schematic illustration of specific uptake of QD-Apt(Dox) conjugates into target cancer cell through PSMA mediate endocytosis. The release of Dox from the QD-Apt(Dox) conjugates induced the recovery of fluorescence from both QD and Dox ("ON" state), thereby sensing the intracellular delivery of Dox and enabling the synchronous fluorescent localization and killing of cancer cells. (c) & (d) Confocal laser scanning microscopy images of PSMA-expressing LNCaP cells after incubation with 100 nM QD-Apt(Dox) conjugates for 0.5 h at 37 °C, washing two times with PBS buffer, and further incubation at 37 °C for (c) 0 h and (d) 1.5 h. Dox and QD are shown in red and green, respectively, and the lower right images of each panel represent the overlay of Dox and QD fluorescence. Reprinted with permission from ref [76].

**Fig. 4.**

(a) Schematic illustration of gold nanoshell synthesis and bioconjugation. (b-d) *In vivo* photothermal ablation with targeted NDP-MSH-PEG-HAuNS to induce selective destruction of B16/F10 melanoma in nude mice. (b) ^{18}F fluorodeoxyglucose PET imaging showed significantly reduced metabolic activity in tumors after photothermal ablation in mice pretreated with NDP-MSH-PEG-HAuNS, but not in mice pretreated with PEG-HAuNS or saline. T, tumor. Arrowheads, tumors irradiated with near-IR light. (c) ^{18}F fluorodeoxyglucose uptake (%ID/g) before and after laser treatment. (d) Histologic assessment of tumor necrosis with H&E staining. Reprinted with permission from ref [122].

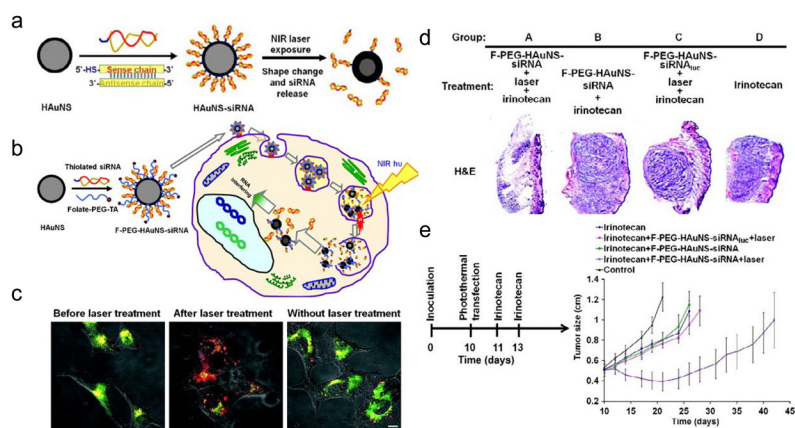


Fig. 5. (a) Scheme for the conjugation and photothermal-activated release of siRNA. (b) Postulated uptake and siRNA release mechanisms of the folated, siRNA-Au shell conjugates. (c) Photothermal-induced endolysosomal escape of Dy547-labeled siRNA. Green, LysoTracker Green-labeled endolysosomes; red, Dy547-labeled siRNA. Scale bar, 10 μm . (d) & (e), effect of p53 siRNA photothermal transfection combined with irinotecan on nude mice bearing HeLa cancer xenografts. (d) Representative micrographic images of tumors stained with H&E. (e) Tumor size versus time curve. Control, tumor-bearing mice did not receive any treatment. Reprinted with permission from ref [123].

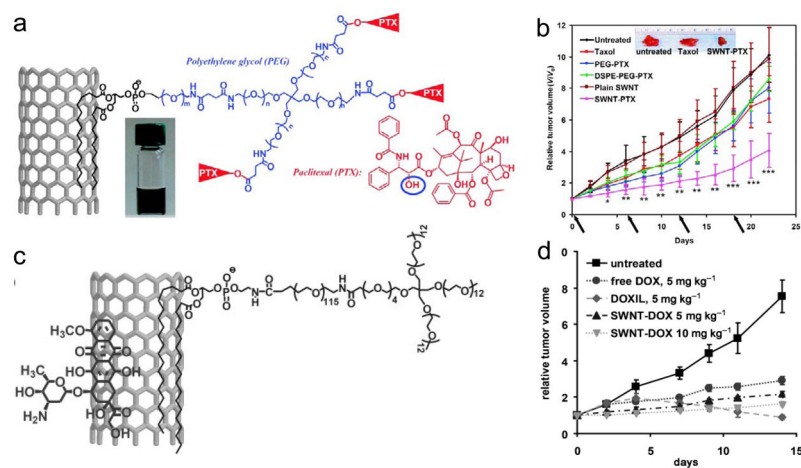


Fig. 6. (a) Schematic illustration of the PTX conjugation to SWNT functionalized by phospholipids with branched PEG chains. (b) Tumor growth curves of 4T1 tumor-bearing mice that received different treatments. (c) Scheme for DOX-SWNT complex formation. (d) Tumor growth curves. Raji-tumor-bearing SCID mice were treated with different DOX formulations. Reprinted with permission from ref [156] and [158].

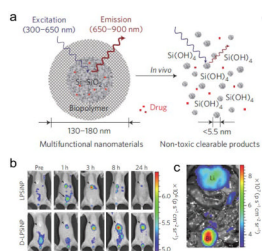
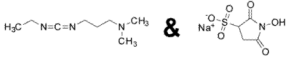
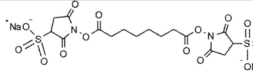
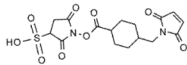


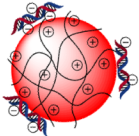

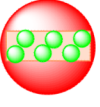



Fig. 7. (a) Schematic diagram depicting the structure and *in vivo* degradation process of the silica nanoparticles. (b) *In vivo* images of luminescent porous silicon nanoparticles (LPSiNPs) and dextran coated LPSiNPs (D-LPSiNPs). The mice were imaged at multiple time points after intravenous injection of LPSiNPs and D-LPSiNPs (20 mg/kg). Arrowheads and arrows with solid lines indicate liver and bladder, respectively. (c) *In vivo* image showing the clearance of a portion of the injected dose of LPSiNPs into the bladder, 1 h post-injection. Li and Bl indicate liver and bladder, respectively. Reprinted with permission from ref [188].

Table 1

Commonly used techniques to load functional entities onto nanoplatforms

| Common Bioconjugation Techniques | | | |
|---|---|--|---|
| Moieties to be coupled (nanoparticle and drug molecule/targeting motif) | | Crosslinkers or mediators | Final conjugates |
| R1-NH₂ | R2-COOH |  | R1-NH-CO-R2 |
| R1-NH₂ | R2-NH₂ |  | R1-NH-CO-(CH₂)₆-CO-NH-R2 |
| R1-NH₂ | R2-SH |  | R1-NH-CO-(CH₂)₆-CO-NH-R2 |
| R1-biotin | R2-biotin |  (Streptavidin or NeutrAvidin) | R1-biotin  biotin-R2 |
| Other Drug Loading Strategies | | | |
| Electrostatic Interaction | Co-loading nanoparticles and drug molecules into polymer/protein matrices | Adsorption into mesoporous nanostructures | π-π stacking |
|  |  |  |  |